Plasticity in striatal dopamine release is governed by release-independent depression and the dopamine transporter

Mark D. Condon[1], Nicola J. Platt[1], Bradley M. Roberts[1], Min-Yee Tseu[1], Stefania Vietti-Michelina[1], Sarah Threlfell[1,2] and Stephanie J. Cragg[1,2]*

[1]Department of Physiology, Anatomy and Genetics, Parks Road, University of Oxford, OX1 3PT, UK

[2]Oxford Parkinson's Disease Centre, Oxford, OX1 3PT

*Author for Correspondence: Stephanie.cragg@dpag.ox.ac.uk, +44 1865 282513

Short Title: Short-term plasticity in dopamine release

Keywords: Dopamine, striatum, release probability, dopamine release, short-term plasticity, short-term depression, short-term facilitation, dopamine transporter, release-independent depression, axonal excitability, voltammetry

Key Findings:

- Short-term plasticity in dopamine release is only weakly governed by Ca^{2+} and initial release
- Short-term depression is strongly dependent on regulation of axonal excitability
- The DAT determines short-term plasticity and drives short-term depression
- DAT governs the balance between release-dependent and release-independent mechanisms

Abstract

Action potentials in mesostriatal dopamine (DA) neurons encode the motivational value of salient stimuli. DA neurons possess extensively branched axonal arbours, and how action potentials are converted to DA output will be influenced dynamically and critically by axonal mechanisms that are poorly understood. We explored the role for mechanisms governing release probability and axonal excitability in determining short-term plasticity (STP) of DA release, using fast-scan cyclic voltammetry in *ex vivo* mouse striatum. The brief short-term facilitation (STF) and longer short-term depression (STD) seen were only weakly dependent on initial release. Rather, STP was strongly governed by release-independent mechanisms that involved K^+-dependent axonal excitability and surprisingly, the dopamine transporter (DAT), particularly in dorsal striatum. The DAT acts as a master regulator of DA STP, governing the balance between release-dependent and release-independent mechanisms that also show region-specific gating.

Introduction

Dopamine (DA) release in the striatum plays key roles in action selection and behavioural reinforcement, and is dysregulated in diverse disorders including Parkinson's disease and addictions. DA neurons generate action potentials (APs) at a range of frequencies, firing tonically below 10 Hz, and intermittently in short bursts with instantaneous frequencies of up to approximately 40 Hz (1-6). Bursts occur in response to salient environmental stimuli predicting reward value or action signals (6-8). However, the extent to which AP activity is conveyed into striatal DA release remains unclear: DA axons are important sites for local regulation of DA output (9-12) which shows strong short-term plasticity (STP) and distorts the relationship between activity and DA output (11, 13-16).

Despite classical accounts of axons as simple high-fidelity cables, neurotransmitter release from CNS axons is shaped by factors that regulate AP propagation and axonal excitability such as axonal morphology, and the expression of ion channels, presynaptic receptors and other diverse mechanisms that regulate neurotransmitter release probability and STP (17). Axons of DA neurons are remarkable; they comprise vast,

41 extensively branched arbours (18, 19), and therefore axonal properties are likely to be particularly important
42 in governing striatal DA output. One major axonal influence is input from striatal cholinergic interneurons
43 onto nicotinic receptors (nAChRs) which influence the pattern of DA release and promote short-term
44 depression (STD) (11, 14, 20-22). In the absence of nAChR activation, DA release shows an underlying
45 spectrum of STP ranging from short-term facilitation (STF) to STD (11, 14, 21, 23, 24) but the underlying
46 mechanisms are poorly understood. There is evidence that STP might be only weakly related to initial levels
47 of release (16, 23, 24).

48 Here, we delineate the roles of three types of intrinsic mechanisms on DA axons that could underlie
49 STP of DA release. We examine, firstly, the role for initial release, a proxy for probability of release (P_r);
50 secondly, the role for K^+-dependent processes such as axonal membrane excitability and repolarization; and
51 thirdly, whether STP can be influenced by the dopamine transporter (DAT). Besides mediating DA uptake,
52 the DAT generates a depolarising transport-coupled conductance in midbrain DA neurons (25, 26), and limits
53 vesicular release through suggested interactions with synaptic vesicle proteins (27, 28). Thus, the DAT has
54 the potential to govern STP of DA release via regulation of axonal excitability and/or P_r.

55 We reveal that initial P_r plays a limited role in STP which is largely release-independent, except on
56 the shortest of timescales when STF operates. We identify that STD is strongly determined by membrane
57 excitability, particularly in dorsal striatum, and that the DAT drives STF and STD, effectively clamping release
58 at physiological inter-pulse intervals. We propose a region-specific hierarchy of interacting drivers of STP,
59 overseen by the DAT, with the DAT promoting release-insensitive over release-dependent mechanisms.

Results

Patterns of short-term plasticity at DA release sites are region-specific and weakly release-dependent

We assessed STP of DA release in acute coronal striatal slices evoked using pairs of local electrical pulses. All experiments were conducted without the confounding effects of evoked striatal ACh by inclusion of nAChR antagonist DHβE (1 μM) throughout. Inclusion of nAChR antagonists during local stimulation also makes evoked DA release in *ex vivo* slice resemble DA release evoked *in vivo* by midbrain or medial forebrain bundle stimulation: sensitivity to frequency as seen *in vivo* (29, 30) is unmasked in slices by nAChR inhibition (14, 31). The ratio of DA release evoked by the second pulse in a pair of pulses compared to a single pulse (paired-pulse ratio, PPR) varied with inter-pulse intervals (IPI) of 10-200 ms in dorsolateral striatum (CPu) (**Fig. 1A,C**) and in nucleus accumbens core (NAc) (**Fig. 1B,C**). In both regions, PPR decreased with increasing IPI. Short-term facilitation (STF, PPR>1) was observed at the shortest IPIs (10 ms in CPu, 10-25 ms in NAc), whereas short-term depression (STD) (PPR<1) was observed at longer IPIs (≥ 25 ms in CPu, >40 ms in NAc), as shown previously (14, 32). In CPu, STD at IPIs ≥ 25 ms was significantly more pronounced than in NAc (**Fig. 1C,** Two-way ANOVA, region x IPI interaction, $F_{4,25} = 4.195$, $P = 0.010$, $n = 7$). STP of DA release therefore shows strong STD in both CPu and NAc, and to a greater extent in CPu, which suggests region-specific gating of STP.

PPR is usually inversely related to initial release probability (P_r) at central synapses, resulting in STF when P_r is low, and STD when P_r is high (33-36). STF at these synapses consists of several temporally-overlapping processes with a range of time constants from 30 – 500 ms (37). An inverse relationship between PPR and single pulse release has been seen in CPu for very short IPI of 10 ms but not at 100 ms (23), suggesting that STP of DA release might reflect initial P_r at only very short intervals. We probed the relationship between PPR and the DA release evoked by a single pulse (as a proxy of initial P_r) in CPu and in NAc across a population of release sites that exhibited a 10-fold range in $[DA]_o$ evoked by a single pulse (1p

84 $[DA]_o$). We found an inverse relationship between 1p $[DA]_o$ and PPR for IPI of 10 ms in both CPu and NAc,
85 and for 40 ms in NAc only, but in neither region at intervals of 100 ms (**Fig. 1D,** linear regressions, 10 ms,
86 CPu: β = -0.79 ± 0.14 [95% CI: -1.08 to -0.50], $F_{1,33}$ = 30.9, *P* = 3.56 x 10^{-6}, *n* = 35; NAc: β = -0.52 ± 0.19 [95% CI:
87 -0.93 to -0.11], $F_{1,17}$ = 7.136, *P* = 0.016, *n* = 19; 40 ms, CPu, *P* = 0.152, *n* = 35; NAc 95% CI: -0.38 to -0.001], $F_{1,}$
88 $_{17}$ = 4.489, *P* = 0.049, *n* = 19; 100 ms, CPu: *P* = 0.122, n = 35; NAc: *P* = 0.917, n = 19). These data suggest that
89 DA PPR is a function of P_r at only very short intervals and specifically, only at those intervals at which we
90 observe a STF. These data also confirm that STP of DA release is dominated by STD at all but the shortest
91 intervals (≤25 ms) and indicate that PPR at physiological IPIs (≥40 ms) is not strongly influenced by P_r. Taken
92 together these findings suggest that STP might be governed by release-dependent mechanisms at short
93 intervals, but by mechanisms unrelated to initial release at longer physiological intervals, across striatum.

94 We tested whether this expression of STD could be explained by activation of inhibitory D2-type
95 autoreceptors (D2Rs). We prevented activation of D2Rs with the D2/D3-receptor antagonist L741,626.
96 L741,626 (1 µM) did not appear to influence peak $[DA]_o$ (**Fig. 1E**) and did not significantly alter PPR at IPIs up
97 to 200 ms in either CPu or NAc (**Fig. 1F**, Two-way ANOVA, CPu: *P* = 0.420, n= 5, NAc: *P* = 0.2197, n = 6),
98 consistent with previous findings that D2Rs modify release at only longer IPI (>200 ms) (13, 38-40). These
99 findings show that STD at these intervals is not explained by D2R activation.

100 STP is shaped by release-dependent facilitation and release-independent depression

101 To test directly whether STP is governed by P_r, we varied P_r at a given release site by varying the extracellular
102 concentration of Ca^{2+} ($[Ca^{2+}]_o$) between 1.2 and 3.6 mM. $[DA]_o$ evoked by 1p was strongly dependent on
103 $[Ca^{2+}]_o$, in both CPu and NAc (**Fig. 2A,B**) as expected, and varying $[Ca^{2+}]_o$ had a stronger outcome on 1p $[DA]_o$
104 in CPu than in NAc (**Fig. 2C**, Two-way ANOVA, $[Ca^{2+}]_o$ x region interaction, $F_{2,20}$ = 17.25, *P* = 4.43 x10^{-5}, *n* = 6),
105 consistent with previous findings (24). However, despite large changes in 1p-evoked DA release (2.5 to 4-
106 fold), $[Ca^{2+}]_o$ had only modest effects on PPR. In CPu, a trend towards an inverse relationship at 10 ms IPI did
107 not reach significance (**Fig. 2D,F**, Two-way ANOVA, *P* = 0.604, n = 4), while in NAc, PPR varied inversely with
108 $[Ca^{2+}]_o$ at short intervals, reaching significance at only 10 ms IPI (**Fig. 2E,F,** Two-way ANOVA, IPI x $[Ca^{2+}]_o$

109 interaction, $F_{8,30}$ = 4.497, *P* = 0.001, *n* = 3). Therefore, the effects of varying P_r on PPR are subtle and limited
110 to very short IPIs, revealing that STP of DA release is only weakly governed by classic presynaptic release-
111 dependent mechanisms, and suggesting that other mechanisms might be important.

112 We noted also that the greater range in PPR seen in NAc than in CPu across different $[Ca^{2+}]_o$ occurred
113 over a smaller range of 1p $[DA]_o$ than in CPu: there was an apparently stronger relationship between initial
114 release and STP in NAc than CPu (**Fig. 2F**). The difference in STP between CPu and NAc cannot therefore be
115 attributed to a difference in the sensitivity of initial P_r to $[Ca^{2+}]_o$ (see Fig. 2C). Thus, STP of DA release can be
116 governed only partly by $[Ca^{2+}]_o$-dependent processes, and must involve additional participating mechanisms
117 that are not modulated by P_r which, by definition, can be referred to as release-insensitive (or release-
118 independent).

119 To confirm that STD and insensitivity to $[Ca^{2+}]$ are intrinsic properties of DA axons, and are not a
120 result of co-activation of an undefined input to DA axons, we used optogenetic stimulation of DA axons to
121 selectively evoke DA release. In striatum from heterozygote $DAT^{IRES\text{-}Cre}$ mice expressing ChR2-eYFP, a brief
122 light flash (2 ms, 473 nm wavelength) evoked $[DA]_o$ transients that varied with varying $[Ca^{2+}]_o$ (**Fig. 2G**) and
123 with a steeper $[Ca^{2+}]_o$ concentration-response curve in CPu than in NAc (**Fig. 2H**, nonlinear regression, CPu:
124 R^2 = 0.91, n = 3, NAc: R^2 = 0.94, n = 3, comparison of fits: $F_{4,118}$ = 5.94, *P* = 2 x 10^{-4}), as seen for electrically
125 evoked DA release. Furthermore, at an interval of 40 ms, at which ChR2 can reliably drive repeat spiking in
126 DA neurons (1) and can be followed by the release of DA (11), PPR was greater in NAc than in CPu as
127 observed using electrical stimulation (see Fig. 1C) and moreover, there was no inverse relationship between
128 PPR and 1p $[DA]_o$ (**Fig. 2I,** linear regression, CPu: *P* = 0.874, n = 3, NAc: *P* = 0.286, n = 3). These data confirm
129 that STD is not attributable to concurrent activation of other inputs. For subsequent experiments, we chose
130 to electrical over optogenetic stimulation (with nAChR inhibitors included throughout) to avoid confounding
131 effects of ChR2 conductances on Ca^{2+} entry.

132 ## A release-insensitive mechanism of short-term depression is controlled by K^+-dependent gating

133 We next tested whether STD is driven by mechanisms related to membrane excitability by varying $[K^+]_o$.
134 Varying $[K^+]_o$ can alter membrane potential and/or rate of repolarisation through the Nernstian driving forces
135 underlying K^+-mediated currents (41) and/or through K^+-dependent inhibition of K^+-channel inactivation (42).
136 Reduced $[K^+]_o$ can favour membrane hyperpolarisation, and faster repolarisation between pulses promoting
137 de-inactivation of Na^+ channels, but can also promote inactivation of K^+-channels, leading to use-dependent
138 depolarisation and enhanced Na^+-channel recruitment. In either case, recruitment of voltage-gated Na^+
139 channels at a subsequent depolarising event will be altered.

140 We found that varying $[K^+]_o$ (1.25 - 7.5 mM) did not change 1p $[DA]_o$ in either CPu (**Fig. 3A**) or NAc
141 (**Fig. 3B**) but significantly modulated STP (**Fig. 3A-D**). In CPu, PPR varied inversely with $[K^+]_o$ at all IPIs, with
142 STD minimized at lowest $[K^+]_o$ (**Fig. 3C**, Two-way ANOVA, $[K^+]_o$ x IPI interaction, $F_{8,30} = 7.66$, $P = 1.53 \times 10^{-5}$, $n =$
143 3). In NAc, the effect of $[K^+]_o$ on PPR was less evident than in CPu, but showed an overall significance (**Fig. 3D**,
144 Two-way ANOVA, main effect of $[K^+]_o$, $F_{2,30} = 15.15$, $P = 2.83 \times 10^{-5}$, $n = 3$). Since we observed no effect of $[K^+]_o$
145 on 1p $[DA]_o$, these effects on PPR were unrelated to initial P_r at either short (10 ms) or longer (100 ms) IPI
146 (**Fig. 3E,** vertical slopes). These findings demonstrate directly that STP of DA release can be dissociated from
147 initial P_r, i.e. there is a release-independent STP. Furthermore, they suggest that STD is governed by K^+-
148 dependent membrane polarisation/excitability particularly in CPu.

149 ## K^+-dependent gating of short-term depression requires axonal K_v channels

150 To identify whether the control of STP by $[K^+]_o$ is accounted for by voltage-gated K channels (K_v) channels we
151 tested whether the effects of $[K^+]_o$ on PPR could be substituted for, and prevented by, the broad-spectrum
152 blocker 4-aminopyridine (4-AP). We hypothesised that by reducing K_v conductances, 4-AP should promote
153 STD and prevent effects of further changes in $[K^+]_o$. In CPu, 4-AP (100 µM), unlike changes in $[K^+]_o$ alone,
154 profoundly increased 1p $[DA]_o$ (**Fig. 4A, B**, Two-way ANOVA, main effect of 4-AP: $F_{1,3} = 33.63$, $P = 0.010$, $n =$
155 4). This effect is consistent with the widening of the action potential by 4-AP seen in DA neurons (43) which

156 will increase Ca^{2+} entry and neurotransmitter release for a single stimulus. In addition, 4-AP, similar to the
157 effects of high $[K^+]_o$ (see Fig. 3), but unlike high $[Ca^{2+}]_o$ (see Fig. 2), reduced PPR at all IPIs, and also prevented
158 the effects of changing $[K^+]_o$ on PPR (**Fig. 4C, 4D,** Two-way ANOVA, 4-AP x $[K^+]_o$ interaction, $F_{1, 12} = 6.003$, $P =$
159 0.031, $n = 4$). These findings indicate that inhibition of K_v channels promotes STD, and suggest conversely
160 that enhanced K_v currents relieve STD, and suggest that hyperpolarizing/repolarizing conditions limit STD and
161 promote subsequent release.

162 In NAc, we observed no significant effect of 4-AP on 1p $[DA]_o$ (**Fig. 4E,F**, Two-way ANOVA, $P = 0.266$,
163 n = 3). 4-AP did decrease PPR at all IPIs, although there was no effect of varying $[K^+]_o$ in control conditions or
164 in the presence of 4-AP (**Fig. 4G, H**). These findings verify further that STD can be distinct from the effects on
165 initial P_r and that STD is underpinned by K_v-gated regulation of axonal excitability.

166 K^+-dependent gating does not alter release-dependence of STP

167 We investigated whether $[K^+]_o$-dependent STD could be a limiting factor that prevents STP of DA release
168 from responding to changes in P_r. We explored whether a relief of STD in low $[K^+]_o$ could unmask a greater
169 sensitivity of STP to changes in P_r driven by variation in $[Ca^{2+}]_o$. In CPu, 1p-evoked $[DA]_o$ varied with $[Ca^{2+}]_o$ in
170 a similar manner in 1 mM and 5 mM $[K^+]_o$ (**Fig. 5A-C**) and although PPRs were higher when $[K^+]_o$ was lower
171 (**Fig. 5D**) (as seen in Figs. 3C, 4C), there was no significant interaction between $[K^+]_o$ and $[Ca^{2+}]_o$ at IPIs of
172 either 10 ms or 100 ms (**Fig. 5D**, Two-way ANOVA, 10 ms IPI: $P = 0.086$, 100 ms IPI: $P = 0.654$, n = 10). By
173 limiting STD, we did not enhance Ca^{2+}-dependent modulation of STF or reveal a relationship between STD
174 and P_r in CPu.

175 In NAc, 1p $[DA]_o$ varied with $[Ca^{2+}]_o$ in a manner that did not depend on $[K^+]_o$ (**Fig. 5E-G**).
176 Furthermore, there was no significant interaction between the effects of $[K^+]_o$ and $[Ca^{2+}]_o$ on PPR at either 10
177 ms or 100 ms IPI (**Fig. 5H**, Two-way ANOVA, 10 ms IPI: $P = 0.963$, 100 ms IPI: $P = 0.883$, n = 7). The release-
178 independent mechanism through which $[K^+]_o$ modulates STP does therefore not apparently mask classical

179 roles for Ca^{2+} in STP, in either CPu or NAc. This suggests that an additional mechanism may operate to limit
180 the Ca^{2+}-dependence of STP besides K_v-regulation of axonal excitability and polarization.

181 The dopamine transporter regulates STP of dopamine release

182 The dopamine transporter (DAT) has previously been shown to limit DA release (27, 28) by a mechanism that
183 is independent of DA transport (44-46), suggesting that the DAT might play a key role in regulating P_r
184 alongside its role in the uptake of DA. The DAT is also known to mediate electrogenic currents during DA
185 binding and transport (25, 47) that have been shown to modulate the membrane potential of DA neurons *in*
186 *vitro* (26). We therefore investigated whether DAT in striatum regulates STP.

187 We explored PPR in the presence of a range of uptake inhibitors. We found that the monoamine
188 uptake inhibitors cocaine and methylphenidate (MPH) and the DAT-selective inhibitor nomifensine
189 significantly altered the pattern of STP in a common manner. Cocaine (5 µM), MPH (5 µM) or nomifensine
190 (10 µM) increased the peak amplitude and decreased the rate of decay of $[DA]_o$ transients in CPu and NAc in
191 keeping with DA re-uptake inhibition (**Fig. 6A,C,G,I**). Furthermore, they significantly altered STP. In CPu, DAT
192 inhibition prevented STF and significantly relieved STD (Cocaine: **Fig. 6A,B**, Two-way ANOVA, cocaine x IPI
193 interaction, $F_{4, 30} = 11.97$, $P = 6.24 \times 10^{-6}$, $n = 4$, MPH: **Fig. 6C,D**, Two-way ANOVA, MPH x IPI interaction, $F_{4, 40}$
194 $= 5.316$, $P = 0.002$, $n = 5$; Nomifensine: **Fig. 6E,F**, Two-way ANOVA, nomifensine x IPI interaction, $F_{4, 80} =$
195 21.12, $P = 6.5 \times 10^{-12}$, $n = 3$). These findings indicate that the DAT is a key regulator of STP of DA release. At
196 shortest IPI, DAT promotes STF, whereas at longer IPI, DAT clamps release to promote STD in CPu.

197 We ruled out potential local anaesthetic actions of cocaine on voltage-gated Na^+ channels (VGSCs),
198 since lignocaine (10 µM), an inhibitor of VGSCs, did not significantly alter STP (**Fig. S1**), consistent with
199 reports that cocaine does not inhibit VGSCs at the concentration used in this study (48).

200 In NAc, cocaine and MPH (we did not test nomifensine in this region) prevented STF at 10 ms IPI (**Fig.**
201 **6G,H,** Two-way ANOVA, cocaine x IPI interaction, $F_{4, 30} = 7.884$, $P = 1.82 \times 10^{-4}$, $n = 4$; MPH: **Fig 6I,J,** Two-way
202 ANOVA, MPH x IPI interaction, $F_{4, 20} = 3.986$, $P = 0.016$, $n = 3$) but in contrast to CPu, STD at longer intervals

203 was not relieved. In NAc, the DAT regulated STP at only short interpulse intervals. Since it is at these intervals
204 that STP is related to P_r (see Fig 1), these data suggest that it is the effect of DAT inhibition on promoting DA
205 release that underlies its effects on STP at short intervals in NAc.

206 We tested whether the effects of DAT inhibition on STP were dependent on synapsin III, since it has
207 been suggested that this protein might mediate the role of the DAT in vesicle segregation and in limiting
208 release (27). However, we found that the effects of cocaine persisted in mice lacking synapsin III (**Fig. S2**),
209 indicating that the DAT regulates STP via a synapsin III-independent or a redundant mechanism.

210 The DAT limits release-dependence of STP in CPu

211 Since the DAT operates a clamp on DA release in CPu that drives STD, we tested whether the DAT might
212 prevent STP from being release-dependent. We explored whether inhibition of the DAT could expose a
213 stronger relationship between $[Ca^{2+}]_o$ and PPR in CPu. We found that whereas there was no effect on PPR of
214 changing $[Ca^{2+}]_o$ in the absence of cocaine (**Fig. 7A,B**, Two-way ANOVA, $P = 0.209$, n = 4), in the presence of
215 cocaine by contrast there was a significant effect of $[Ca^{2+}]_o$: PPR at IPIs of 10-40 ms were significantly
216 elevated in 1.2 versus 2.4 mM $[Ca^{2+}]_o$ (**Fig. 7A,C-E**, Two-way ANOVA, $[Ca^{2+}]_o$ x IPI interaction, $F_{3, 24} = 6.137$, $P =$
217 0.003, $n = 4$). There was a significantly stronger effect of $[Ca^{2+}]_o$ on PPR in the presence of cocaine than in
218 control conditions at 25 ms (**Fig. 7D;** Two-way ANOVA, cocaine x $[Ca^{2+}]_o$ interaction; $F_{1, 12} = 7.86$; $P = 0.016$; n
219 $= 4$) and 40 ms IPI (**Fig. 7D**; Two-way ANOVA, cocaine x $[Ca^{2+}]_o$ interaction; $F_{1, 12} = 4.72$, $P = 0.050$, $n = 4$), but
220 not at 10 ms or 100 ms IPI. These effects were not due to a potential electrochemical change in dopamine
221 adsorption/desorption kinetics at the electrode that might occur with a change in divalent cations, since
222 these effects of cocaine were maintained when the reduction in $[Ca^{2+}]_o$ was compensated by equimolar
223 substitution with Mg^{2+} (**Fig. S3**)**.** Inhibition of the DAT therefore relieves the clamp on a relationship between
224 PPR and initial release, suggesting that the DAT drives STD and limits the release-dependence of STP.

225 ## The DAT maintains K^+-dependent gating of STP

226 We noted that the effect of DAT inhibitors on relieving STD resembled the effect of low $[K^+]_o$. Since inhibition
227 of the DAT might prevent DAT-mediated depolarising conductances and lead to axonal hyperpolarisation, we
228 tested whether cocaine and low $[K^+]_o$ relieve STD via an overlapping mechanism i.e. promoting membrane
229 hyperpolarisation/repolarisation. To test this, we identified whether cocaine precluded the effect of varying
230 $[K^+]_o$ (1 vs 5 mM) on STP, in CPu and NAc.

231 In CPu, in the absence of cocaine, PPR were elevated in lower $[K^+]_o$ (**Fig. 8A,B**, Two-way ANOVA, main
232 effect $[K^+]_o$, $F_{1, 18} = 20.47$, $P = 2.62 \times 10^{-4}$, $n = 4$) as seen in Fig. 3. Cocaine increased 1p-evoked peak $[DA]_o$ to a
233 similar extent in 5 mM versus 1 mM $[K^+]_o$ (**Fig. 8C**) but prevented the effect on PPR of varying $[K^+]_o$ (**Fig. 8D**,
234 Two-way ANOVA, $[K^+]_o$ x cocaine interaction, $F_{1, 12} = 7.686$, $P = 0.017$, $n = 8$). The limited ability of low $[K^+]_o$ to
235 increase PPR was not due simply to some ceiling effect such as depletion of DA due to increased P1 release
236 in cocaine, since cocaine also prevented the opposite effects of a raise in $[K^+]_o$ (to 7.5 mM) from decreasing
237 PPR (**Fig. S4**).

238 In NAc, PPR were slightly elevated in lower $[K^+]_o$ (**Fig. 8E,F**, Two-way ANOVA, main effect $[K^+]_o$, $F_{1,12} =$
239 6.840, $P = 0.023$, $n = 3$). Cocaine increased 1p-evoked peak $[DA]_o$ to a similar extent in 5 mM versus 1 mM
240 $[K^+]_o$ (**Fig. 8G**), and, as in CPu, prevented the effect of varying $[K^+]_o$ on PPR (**Fig. 8F,H**, Two-way ANOVA, $[K^+]_o$ x
241 cocaine interaction, $F_{1,8} = 6.756$, $P = 0.032$, $n = 3$). The effects of $[K^+]_o$ on STP are therefore abolished by
242 cocaine, suggesting that STP is regulated by a pathway common to $[K^+]_o$ and DAT function. DAT function
243 appears to regulate STP in a manner that supports $[K^+]_o$-dependent modulation.

244 # Discussion

245 We explored the major intrinsic mechanisms operating on DA axons that govern the dynamic probability of
246 DA release, in dorsal and ventral striatum. We show that STP is governed in only a limited manner by Ca^{2+}-
247 dependent regulation of release probability, which participates subsequently in determining STF but not
248 STD, and to greater extent in ventral than dorsal striatum. We reveal that release-independent mechanisms

249 drive strong STD of release, particularly in dorsal striatum, where axonal excitability and the DAT are major
250 players and dominate over Ca^{2+}-dependent gating. The DAT appears to be a master regulator that sets DA P_r
251 and its resulting STF, and clamps release leading to release-independent STD particularly in dorsal striatum.
252 The differences seen between regions could in turn lead to different DA outputs in dorsal and ventral
253 striatum in response to changes in AP firing, and could underpin different outcomes of striatal modulatory
254 inputs.

255 Calcium-dependent facilitation

256 Studies of STP at central synapses commonly demonstrate an inverse relationship to P_r; facilitation is
257 typically observed when P_r is low, and depression when P_r is high (49). Here, we show that, in NAc, an
258 inverse relationship between STF and P_r could be observed for short IPI corresponding to instantaneous
259 frequencies seen during fast burst firing (~25 Hz), but the strength of STD at lower frequencies was not
260 altered. By contrast, in CPu, changes to DA P_r do not strongly influence STP. There seems to be a limited
261 relationship between factors that influence Ca^{2+} entry, initial P_r as defined here, and the dynamic plasticity of
262 DA release, especially in CPu, where other release-independent mechanisms are particularly influential.

263 These findings also suggest that mechanisms governing STF might operate differently between NAc
264 and CPu. STF at other synapses is often attributed to summation of residual Ca^{2+} (50, 51), or Ca^{2+}-dependent
265 ultrafast recruitment of vesicles (52), and Ca^{2+} dynamics also vary with local Ca^{2+} buffering mechanisms (53).
266 In NAc, we saw that Ca^{2+}-dependent STF plays a stronger role in regulating STP than in CPu, despite a weaker
267 relationship between $[Ca^{2+}]_o$ and P_r than in CPu. These differences in Ca^{2+} -dependence between NAc and
268 CPu could correspond in part to differences in their Ca^{2+} binding proteins. For example, the high-affinity fast
269 Ca^{2+} buffer calbindin-D_{28k} is expressed at 2-3-fold greater levels in DA neurons of ventral tegmental area
270 (VTA) than substantia nigra pars compacta (SNc), which predominantly project to NAc and CPu respectively
271 (54-56). Saturation of calbindin following initial Ca^{2+} entry could increase P_r at subsequent stimulations
272 resulting in enhanced STF, as seen in other neurons (57, 58).

Release-insensitive depression

At longer interpulse intervals (40-200 ms) corresponding to a large range of physiological firing frequencies (5-25 Hz), STP of DA release is dominated by powerful STD. This was not due to D_2 autoreceptor (D2R) activation. STD of release of other neurotransmitters can result from depletion of readily-releasable vesicles (59), but the STD seen here for DA does not seem to be due to depletion. Not only is a low fraction of presynaptic DA estimated to be released after stimulation (13, 16, 60, 61), but moreover STD in the present study was not relieved by reducing initial release (by $[Ca^{2+}]_o$), inconsistent with a depletion mechanism. VGCC inactivation by a Ca^{2+} sensor has been proposed to drive STD at some central synapses (62-64) but since low $[Ca^{2+}]_o$ did not relieve STD for DA release, this mechanism is unlikely to be a critical factor for DA STD.

We show that STD of DA release is not sensitive to the magnitude of initial release (a measure of P_r), and so can be considered a release-insensitive depression. We found, particularly in CPu, that the strength of STD was inversely correlated with $[K^+]_o$, consistent with findings at some other central synapses (65). We found further that we could dissociate mechanisms governing STD from those governing initial release: STD varied with $[K^+]_o$ despite no change in initial P_r. The $[K^+]_o$-dependent modulation of STP was dependent on K_v channels, which regulate terminal excitability and rates of repolarisation in several axon types (66-69) indicating that membrane polarisation is a critical factor in determining STD for DA release.

These findings together suggest that mechanisms regulating Ca^{2+} entry into DA axons will change the overall amplitude of DA signals, but will not change the dynamic contrast in DA signals when DA neurons change their firing frequency, except at very highest frequencies in NAc. Conversely, mechanisms that modulate K^+ conductances or other mechanisms underlying axonal membrane potential and repolarisation, will particularly influence the dynamic contrast in DA signals. Varying $[K^+]_o$ changes the Nernstian driving force for K^+ currents (41), altering the rate of repolarisation at DA axons and therefore the degree of Na^+ channel inactivation, but also alters the rate of K^+ channel inactivation (42) leading to use-dependent changes in membrane potential that will influence Na^+ channel recruitment at the second pulse. We cannot distinguish here which of these opposing mechanisms dominates to govern STP but in either scenario, Na^+-

channel recruitment will be modified and will govern subsequent release events, leading to varying dynamic summation of $[DA]_o$. Other mechanisms that influence Na^+ channel availability might also regulate STP; it is noteworthy in this regard that nAChRs can significantly promote DA release and in turn drive a strong STD that limits the frequency sensitivity in DA signals (11, 14).

The critical role for axonal excitability in DA STD is particularly pertinent given DA axon morphology. Midbrain DA neurons form small diameter, unmyelinated, extensively arborised axons each containing on the order of ~10^4 branch points and ~10^5 varicosities (19, 70). These morphological features will not readily favour reliable conduction of action potentials (71). Changes in $[K^+]_o$ that influence membrane potential/repolarisation are likely to change axonal conduction failure (65, 72) and may therefore influence the fidelity and the extent of action potential propagation through the DA axonal tree. AP propagation or failure could therefore be a key determinant of the STD observed in this study as seen elsewhere (73), and furthermore could then be a mechanism by which the size of the DA axonal arbour invaded and the consequent size of the striatal field modulated by DA could be dynamically adapted by presynaptic activity or neuromodulatory inputs.

Changes in propagation fidelity would also be expected to have a greater limiting effect on release where axonal arbours are more extensive. The axonal arbours formed by DA neurons projecting to CPu are more extensive than those projecting to NAc (18, 19, 74), and in parallel, STP showed stronger dependence on K^+-dependent gating in CPu than in NAc. This association suggests that action potentials in VTA DA neurons might more readily invade a fuller extent of their axonal tree than action potentials in SNc DA neurons, a speculation which could have significant implications for the signal processing performed by these different neurons.

Role of the DAT in STP

Besides curtailing the amplitude and lifetime of $[DA]_o$ through re-uptake (75, 76), DAT function has also been shown to limit DA release (44, 45). The DAT has been suggested to inhibit vesicle mobilisation via

322 interactions with SNARES such as synapsins, with synapsin III indicated as a potential candidate (27, 28).
323 Consistent with a role of the DAT in limiting P_r, our findings reveal that DAT function promotes STF of DA
324 release seen at very short interpulse intervals (up to 25 ms). At longer intervals, corresponding to typical
325 firing frequencies (5-25 Hz), when STP is dominated by release-independent depression, we found that the
326 DAT clamps release which promotes STD in CPu. Our data do not, however, support a key role for the
327 synapsin III isoform in these DAT functions. Through a different mechanism, the DAT supports both initial P_r,
328 STF and STD, in contrast to the effects of changing either $[Ca^{2+}]_o$ or $[K^+]_o$ alone, indicating that the DAT limits
329 initial DA release probability and also ongoing release.

330 The effects of DAT inhibition on STF were surprisingly large given that, under control conditions, the
331 relationship between P_r and STF was weak. This disparity is reconciled by our finding that DAT inhibition
332 unmasked an enhanced Ca^{2+}-dependent modulation of STP, suggesting that the DAT is a critical player that
333 limits the surprisingly poor relationship between P_r and STP. The mechanism for this interplay is unclear, but
334 since the DAT is an electrogenic transporter (77, 78) that mediates a depolarising current (25, 26, 47) and
335 that it can also regulate VGCCs (79), the DAT is likely to influence both axonal excitability and intracellular
336 Ca^{2+} dynamics in DA axons.

337 Both the DAT and $[K^+]_o$ acted to clamp release, and apparently operated through a common
338 mechanism. The effects of the DAT and $[K^+]_o$ in driving STD of DA release could be indicative of depolarising
339 influences that attenuate conduction propagation through the DA axon arbour, since axonal
340 hyperpolarisation and low $[K^+]_o$ can actually promote AP conduction in some neurons (80). It is also possible
341 that the DAT might interact directly with voltage-gated K^+ channels, as suggested from DAT proteome
342 analyses (81), or indirectly through an interaction with D2Rs (82, 83) which regulate DA release via K^+
343 channel activity (84).

344 Thus overall, our findings provide support for the DAT acting to limit vesicular release, and promote
345 STD, but allowing limited STF at short intervals. DAT action explains the limited expected effects of Ca^{2+}-
346 dependent release probability on STP. Our data do not support a synapsin3-dependent inhibition of vesicle

347 recruitment by the DAT, but do not exclude other synapsins that might be involved in DA vesicle recruitment
348 (27), but might point to a direct action on VGCC function. The overlap with DAT effects and those of K^+ and K_v
349 channels on STD indicates that the DAT can also act through mechanisms governing excitability that could
350 include DAT-dependent depolarising conductances and/or Na^{2+} entry that appear to limited Na^+-channel
351 recruitment and promote STD. It is of note that DATs are widely distributed throughout the length of DA
352 axons (85), and are found at locations thought to correspond to both release-active zones and inactive zones
353 (16). Thus DATs could be ideally positioned to act to govern both fiber recruitment for AP propagation in
354 axons as well as vesicle/VGCC recruitment at active zones. Now defined, these hypotheses should be tested
355 directly in future studies.

356 Furthermore, it is well known that DAT function can alter the frequency-dependence of DA release
357 during ongoing activity (23, 30, 32, 86). These effects are consistent with the effects of uptake on
358 extracellular summation between stimuli and also with the role of DAT in the dynamic probability of release
359 we have identified here. The DAT might in turn also be expected to determine the spatial range of striatal DA
360 transmission not only through its established role in limiting the diffusion of extracellular DA away from
361 release sites but also by limiting AP conduction within the axonal arbour and/or the probability of DA
362 release. It is of further note that the apparently greater role for DAT in driving STD in CPu and NAc correlates
363 with the greater striatal density of DAT at more dorsolateral co-ordinates (87), and with greater DAT
364 transcript levels in SNc than VTA neurons (56).

365 In conclusion, we propose a hierarchy of intrinsic mechanisms that control STP of DA release. Within
366 this hierarchy, the DAT represents a 'master regulator' of STP, governing the balance between release-
367 dependent and release-independent mechanisms that differently dominate in dorsal versus ventral striatum.
368 In turn, DAT inhibitors such as cocaine will have profound effects on DA signalling through promoting P_r,
369 relieving STD, and altering the timecourse and spatial field of DA signals.

370 # Materials and Methods

371 ## Animals

372 Experiments were carried out using adult male C57Bl6/J mice (Jackson Laboratories), heterozygote DAT^{IRES_Cre}
373 mice conditionally expressing ChR2, or synapsin-III knockout (S3KO) mice on a C57Bl6/J background. For
374 experiments using optical stimulation of DA axons, male heterozygote DAT-internal ribosome entry site
375 (IRES)-Cre mice were bred from homozygote DAT$^{IRES\text{-}Cre}$ mice on a C57Bl6/J background (B6.SJL-
376 *Slc6a3*$^{tm1.1(cre)Bkmn}$/J, stock # 006660, Jackson Laboratories). S3KO mice were bred as described previously
377 (Feng et al., 2002), and were kindly supplied by Professor HT Kao (Brown University). All procedures were
378 performed in accordance with the Animals in Scientific Procedures Act 1986 (Amended 2012) with ethical
379 approval from the University of Oxford, and under authority of a Project Licence granted by the UK Home
380 Office.

381 ## Surgery

382 Heterozygote DAT$^{IRES\text{-}Cre}$ mice were injected intracerebrally with a Cre-inducible recombinant AAV serotype 5
383 vector containing an inverted gene for channelrhodopsin-2 fused in-frame with a gene encoding enhanced
384 yellow fluorescent protein (pAAV-double floxed-hChR2(H134R)-EYFP-WPRE-pA). Mice were placed in a
385 stereotaxic frame under isoflurane anaesthesia and a craniotomy was made above the injection site. Injections
386 of 1 µL virus were given either unilaterally or bilaterally in either VTA (co-ordinates from Bregma in mm: AP -
387 3.1, ML ±0.5, DV -4.4) or in the SNc (from Bregma in mm: AP -3.5, ML ±1.2, DV -4.0) using a 2.5 µL 33-gauge
388 Hamilton syringe at 0.2 µL/min with a microinjector. Animals were maintained for at least 3 weeks following
389 surgery to allow virus expression in striatum.

390 ## Slice Preparation

391 Striatal slices were prepared as described previously (31, 88). Mice were sacrificed by cervical dislocation and
392 the brains removed and transferred to ice-cold HEPES-based buffer containing in mM: 120 NaCl, 20 $NaHCO_3$,

393 6.7 HEPES acid, 5 KCl, 3.3 HEPES salt, 2 $CaCl_2$, 2 $MgSO_4$, 1.2 KH_2PO_4, 10 glucose, saturated with 95%O_2/5%CO_2.
394 Acute 300 µm thick coronal striatal slices, containing both dorsal striatum (CPu) and nucleus accumbens core
395 (NAc) were prepared in ice-cold HEPES-based buffer and cut using a vibratome (VT1000S or VT1200S; Leica).
396 Slices were kept at room temperature in HEPES-based buffer for 1 hour before being transferred to the
397 recording chamber and superfused at 1.8-2.0 ml/min in bicarbonate buffer-based artificial CSF (aCSF)
398 containing in mM: 124.3 NaCl, 26 $NaHCO_3$, 3.8 KCl, 2.4 $CaCl_2$, 1.3 $MgSO_4$, 1.2 KH_2PO_4, 10 glucose, saturated
399 with 95% O_2/5% CO_2, at 31-33°C. In all experiments, recordings were carried out in the presence of bath-
400 applied dihydro-β-erythroidine (DHβE, 1 µM), an antagonist at β2 subunit-containing nAChRs. Slices were
401 allowed to equilibrate for 30 minutes prior to recording.

402 Voltammetry

403 Evoked extracellular DA concentration ($[DA]_o$) was measured using FCV at carbon-fibre microelectrodes (fibre
404 diameter 7-10 µm, tip length 50-120 µm). A triangular voltage waveform was scanned across the
405 microelectrode (-700 to +1300 mV and back vs Ag/AgCl reference, scan rate 800 V/s) using a Millar
406 voltammeter (Julian Millar, Barts and the London School of Medicine and Dentistry), with a sweep frequency
407 of 8 Hz, as described previously (31). This sampling rate is sufficient to capture the rising and falling phase of
408 the DA transients; faster sampling rates do not change the data interpretations (not illustrated). Evoked
409 currents were confirmed as DA by comparison of the voltammogram with that produced during calibration
410 with applied DA in aCSF (oxidation peak +500-600 mV and reduction peak -200 mV). Currents at the oxidation
411 peak potential were measured from the baseline of each voltammogram and plotted against time to provide
412 profiles of $[DA]_o$ versus time. Electrodes were calibrated in 2 µM DA in each experimental solution used,
413 including all solutions where $[Ca^{2+}]$ was varied, since electrode sensitivity varies with divalent ion
414 concentration (89). Calibration solutions were made immediately before use from stock solution of 2.5 mM
415 DA in 0.1 M $HClO_4$ stored at 4°C.

416 ## Stimulation and experimental design

417 For experiments using electrical stimulation, DA release was evoked using a surface bipolar concentric Pt/Ir
418 electrode (25 µm diameter, FHC) placed approximately 100 µm from the recording electrode. Stimulation
419 pulses of 200 µs duration were applied at 0.6 mA unless described otherwise. In experiments using tissue
420 from $DAT^{IRES\text{-}Cre}$ mice conditionally expressing ChR2 in DA axons, DA release was evoked with 2 ms full-field
421 illumination of the slice with an LED system emitting light at 470 nm wavelength (OptoLED, Cairn Research)
422 as described previously (11). The LED system illuminated an area of 2.2 mm diameter. The current delivered
423 by the LED power supply was set to produce a perimaximal light intensity (i.e. the minimum light intensity
424 able to evoke maximum $[DA]_o$ following a single 2 ms pulse). Since the perimaximal light intensity is
425 dependent on the level of ChR2 expression, which varies between animals, the appropriate current was
426 determined at the beginning of each experiment. Electrical or optical stimulations were delivered every 2.5
427 minutes, after which dopamine release was fully recovered.

428 Release probability P_r for DA as defined here is a composite measure of synaptic P_r (a function of
429 vesicular P_r and the size of the pool of vesicles) and the number of release sites and fibres recruited by the
430 stimulus. Short-term plasticity (STP) in DA release was explored by applying alternating single pulses (1p) or
431 paired pulses (2p) with inter-pulse intervals (IPIs) of 10 ms – 200 ms in pseudorandom order and in triplicate
432 at each recording site. IPIs of 40 to 200 ms fall within the range commonly observed during burst firing in DA
433 neurons *in vivo* (3, 4). IPIs of 10 to 25 ms IPIs have been observed during burst firing in DA neurons (Hyland
434 et al., 2002) but are particularly useful to interrogate short-term facilitation which occurs on this timescale
435 (14, 23). We calculated paired-pulse ratio (PPR) as a measure of STP. We define PPR as the ratio P2/P1,
436 where P1 is peak $[DA]_o$ detected following 1p stimulus and P2 is the peak $[DA]_o$ attributable to the second
437 stimulation. P2 was determined by subtracting the $[DA]_o$ transient including decay phase after a single pulse
438 from the summated paired-pulse recording, and therefore DA decay kinetics are accounted for. We cannot
439 control for variable fiber recruitment at different stimuli, but can control for variable modulation by other

440 local inputs: PPR on the timecourses explored here is not modified by D2 dopamine receptors (see Results),
441 or by GABA receptors (Lopes and Cragg, unpublished observations).

442 Calcium concentration ($[Ca^{2+}]_o$) in aCSF was varied by varying $[CaCl_2]$. In some experiments where
443 stated, a reduction in $[CaCl_2]$ was substituted with an equimolar quantity of $MgCl_2$. However, Ca^{2+}/Mg^{2+}
444 substitution was not routine because other effects of $[Mg^{2+}]_o$ can confound interpretation. Changes in $[Mg^{2+}]$
445 have been shown to alter Ca^{2+} currents through VGCCs (90, 91), alter G-protein-coupled receptor function,
446 including dopamine D2 receptors (92), change the affinity of calbindin binding to Ca^{2+} (93), trigger
447 complexing of Ca^{2+} by ATP (94), and alter the sensitivity of FCV electrodes to DA (89).

448 Where extracellular potassium concentration ($[K^+]_o$) was varied (1.0 - 7.5 mM), changes in osmolarity
449 were corrected by varying $[Na^+]$. The Na^+- and K^+-containing salts present in aCSF were varied as follows (in
450 mM): In experiments with 1 mM $[K^+]_o$, salts were 127.1 NaCl, 1.0 KCl, 0 KH_2PO_4, 1.2 NaH_2PO_4; For 1.25 mM
451 $[K^+]_o$ salts were 128.0 NaCl, 0.05 KCl, 1.2 KH_2PO_4; For 7.5 mM $[K^+]_o$, salts were 121.8 NaCl, 6.3 KCl and 1.2
452 KH_2PO_4. Recordings in control conditions were collected before and after each experimental manipulation at
453 each recording site. Slices were equilibrated in each solution for at least 20 minutes before data were
454 included for analysis. Experiments were carried out in either the dorsal half of the caudate-putamen (CPu) or
455 nucleus accumbens core (NAc), one site per slice. Release is TTX-sensitive.

456 Data analysis

457 Data were acquired and analysed using Axoscope 10.2, 10.5 (Molecular Devices) or Strathclyde Whole Cell
458 Program (University of Strathclyde, Glasgow, UK) and locally-written scripts in Visual Basic for Applications
459 (Microsoft). Data are expressed as mean ± standard error (SEM) and *n* = number of animals (the number of
460 biological replicates). Within a given experiment, technical replicates were usually obtained in at least
461 triplicate before averaging to obtain the value for that experiment. Statistical comparisons were carried out
462 using GraphPad Prism 6 (GraphPad Software Inc.).

463 ## Drugs

464 DHβE and lignocaine were obtained from Tocris Biosciences or Ascent Scientific. Cocaine hydrochloride and
465 nomifensine maleate were obtained from Sigma. Methylphenidate (Ritalin™) was obtained from Novartis. All
466 drugs were dissolved in either de-ionised water, aqueous acid (nomifensine maleate) or ethanol (lignocaine)
467 to make stock aliquots at 1000-10,000x final concentration and stored at -20°C. The final concentration was
468 made up in aCSF immediately before use.

469 **Acknowledgements:** Funding sources: MRC, BBSRC Interdisciplinary Doctoral Training Program, Clarendon
470 Fund, Monument Trust Parkinson's UK Discovery Award, and Christ Church Oxford.

471 **Author contributions:** M.D.C. designed and performed experiments, analysed and interpreted the data, and
472 co-wrote the manuscript. N.J.P. designed and performed experiments, and analysed and interpreted the
473 data. B.M.R, S.V.M. and M.Y.T performed experiments and analysed data. S.T. and S.J.C. supervised the
474 work. S.J.C. designed the experiments, interpreted the data, and co-wrote the manuscript.

475 **Declaration of Interests:** The authors declare no competing interests.

476 **References**

477 1. Cohen JY, Haesler S, Vong L, Lowell BB, Uchida N. Neuron-type-specific signals for reward and
478 punishment in the ventral tegmental area. Nature. 2012;482(7383):85-8.

479 2. Grace AA, Bunney BS. The control of firing pattern in nigral dopamine neurons: single spike firing. J
480 Neurosci. 1984;4(11):2866-76.

481 3. Grace AA, Bunney BS. The control of firing pattern in nigral dopamine neurons: burst firing. J
482 Neurosci. 1984;4(11):2877-90.

483 4. Hyland BI, Reynolds JNJ, Hay J, Perk CG, Miller R. Firing modes of midbrain dopamine cells in the
484 freely moving rat. Neuroscience. 2002;114(2):475-92.

485 5. Pan WX, Schmidt R, Wickens JR, Hyland BI. Dopamine Cells Respond to Predicted Events during
486 Classical Conditioning: Evidence for Eligibility Traces in the Reward-Learning Network. J Neurosci.
487 2005;25(26):6235-42.

488 6. Jin X, Costa RM. Start/stop signals emerge in nigrostriatal circuits during sequence learning. Nature.
489 2010;466(7305):457-62.

490 7. Matsumoto M, Hikosaka O. Two types of dopamine neuron distinctly convey positive and negative
491 motivational signals. Nature. 2009;459(7248):837-41.

492 8. Schultz W. Responses of midbrain dopamine neurons to behavioral trigger stimuli in the monkey.
493 Journal of neurophysiology. 1986;56(5):1439-61.

494 9. Sulzer D, Cragg SJ, Rice ME. Striatal dopamine neurotransmission: Regulation of release and uptake.
495 Basal Ganglia. 2016;6(3):123-48.

496 10. Hamid AA, Pettibone JR, Mabrouk OS, Hetrick VL, Schmidt R, Vander Weele CM, et al. Mesolimbic
497 dopamine signals the value of work. Nat Neurosci. 2016;19(1):117-26.

498 11. Threlfell S, Lalic T, Platt NJ, Jennings KA, Deisseroth K, Cragg SJ. Striatal dopamine release is triggered
499 by synchronized activity in cholinergic interneurons. Neuron. 2012;75(1):58-64.

500 12. Cachope R, Mateo Y, Mathur BN, Irving J, Wang HL, Morales M, et al. Selective activation of
501 cholinergic interneurons enhances accumbal phasic dopamine release: setting the tone for reward
502 processing. Cell Rep. 2012;2(1):33-41.

503 13. Cragg SJ. Variable Dopamine Release Probability and Short-Term Plasticity between Functional
504 Domains of the Primate Striatum. J Neurosci. 2003;23(10):4378-85.

505 14. Rice ME, Cragg SJ. Nicotine amplifies reward-related dopamine signals in striatum. Nat Neurosci.
506 2004;7(6):583-4.

507 15. Montague PR, McClure SM, Baldwin PR, Phillips PEM, Budygin EA, Stuber GD, et al. Dynamic gain
508 control of dopamine delivery in freely moving animals. J Neurosci. 2004;24(7):1754-9.

509 16. Liu C, Kershberg L, Wang J, Schneeberger S, Kaeser PS. Dopamine Secretion Is Mediated by Sparse
510 Active Zone-like Release Sites. Cell. 2018;172(4):706-18.e15.

511 17. Debanne D. Information processing in the axon. Nature Rev Neurosci. 2004;5(4):304-16.

512 18. Aransay A, Rodríguez-López C, García-Amado M, Clascá F, Prensa L. Long-range projection neurons of
513 the mouse ventral tegmental area: a single-cell axon tracing analysis. Front Neuroanat. 2015;9:59-.

514 19. Matsuda W, Furuta T, Nakamura KC, Hioki H, Fujiyama F, Arai R, et al. Single nigrostriatal
515 dopaminergic neurons form widely spread and highly dense axonal arborizations in the neostriatum. J
516 Neurosci. 2009;29(2):444-53.

517 20. Collins AL, Aitken TJ, Greenfield VY, Ostlund SB, Wassum KM. Nucleus Accumbens Acetylcholine
518 Receptors Modulate Dopamine and Motivation. Neuropsychopharmacol. 2016;41:2830-8.

519 21. Zhang H, Sulzer D. Frequency-dependent modulation of dopamine release by nicotine. Nat Neurosci.
520 2004;7(6):581-2.

521 22. Wang L, Shang S, Kang X, Teng S, Zhu F, Liu B, et al. Modulation of dopamine release in the striatum
522 by physiologically relevant levels of nicotine. Nat Commun. 2014;5:3925.

523 23. Jennings KA, Platt NJ, Cragg SJ. The impact of a parkinsonian lesion on dynamic striatal dopamine
524 transmission depends on nicotinic receptor activation. Neurobiol Dis. 2015;82:262-8.

525 24. Brimblecombe KR, Gracie CJ, Platt NJ, Cragg SJ. Gating of dopamine transmission by calcium and
526 axonal N-, Q-, T- and L-type voltage-gated calcium channels differs between striatal domains. J Physiol.
527 2015;593(4):929-46.

528 25. Carvelli L, McDonald PW, Blakely RD, Defelice LJ. Dopamine transporters depolarize neurons by a
529 channel mechanism. Proc Natl Acad Sci USA. 2004;101(45):16046-51.

530 26. Ingram SL, Prasad BM, Amara SG. Dopamine transporter-mediated conductances increase
531 excitability of midbrain dopamine neurons. Nat Neurosci. 2002;5(10):971-8.

532 27. Kile BM, Guillot TS, Venton BJ, Wetsel WC, Augustine GJ, Wightman RM. Synapsins differentially
533 control dopamine and serotonin release. J Neurosci. 2010;30(29):9762-70.

534 28. Venton BJ, Seipel AT, Phillips PEM, Wetsel WC, Gitler D, Greengard P, et al. Cocaine Increases
535 Dopamine Release by Mobilization of a Synapsin-Dependent Reserve Pool. Journal of Neuroscience.
536 2006;26(12):3206-9.

537 29. Gonon FG. Nonlinear relationship between impulse flow and dopamine released by rat midbrain
538 dopaminergic neurons as studied by in vivo electrochemistry. Neuroscience. 1988;24(1):19-28.

539 30. Garris PA, Wightman RM. Different kinetics govern dopaminergic transmission in the amygdala,
540 prefrontal cortex, and striatum: an in vivo voltammetric study. J Neurosci. 1994;14(1):442-50.

541 31. Threlfell S, Clements MA, Khodai T, Pienaar IS, Exley R, Wess J, et al. Striatal muscarinic receptors
542 promote activity dependence of dopamine transmission via distinct receptor subtypes on cholinergic
543 interneurons in ventral versus dorsal striatum. J Neurosci. 2010;30(9):3398-408.

544 32. Zhang L, Doyon WM, Clark JJ, Phillips PEM, Dani JA. Controls of Tonic and Phasic Dopamine
545 Transmission in the Dorsal and Ventral Striatum. Molec Pharmacol. 2009;76(2):396-404.

546 33. Debanne D, Guérineau NC, Gähwiler BH, Thompson SM. Paired-pulse facilitation and depression at
547 unitary synapses in rat hippocampus: quantal fluctuation affects subsequent release. J Physiol.
548 1996;491(1):163-76.

549 34. Dobrunz LE, Stevens CF. Heterogeneity of Release Probability, Facilitation, and Depletion at Central
550 Synapses. Neuron. 1997;18(6):995-1008.

551 35. Thomson AM. Molecular frequency filters at central synapses. ProgNeurobiol. 2000;62(2):159-96.

552 36. Wilcox KS, Dichter MA. Paired pulse depression in cultured hippocampal neurons is due to a
553 presynaptic mechanism independent of GABAB autoreceptor activation. J Neurosci. 1994;14(3 Pt 2):1775-88.

554 37. Fisher SA, Fischer TM, Carew TJ. Multiple overlapping processes underlying short-term synaptic
555 enhancement. Trends Neurosci. 1997;20(4):170-7.

556 38. Benoit-Marand M, Borrelli E, Gonon F. Inhibition of dopamine release via presynaptic D2 receptors:
557 time course and functional characteristics in vivo. J Neurosci. 2001;21(23):9134-41.

558 39. Phillips PEM, Hancock PJ, Stamford JA. Time window of autoreceptor-mediated inhibition of limbic
559 and striatal dopamine release. Synapse. 2002;44(1):15-22.

560 40. Schmitz Y, Schmauss C, Sulzer D. Altered dopamine release and uptake kinetics in mice lacking D2
561 receptors. J Neurosci. 2002;22(18):8002-9.

562 41. Balestrino M, Aitken PG, Somjen GG. The effects of moderate changes of extracellular K+ and Ca2+
563 on synaptic and neural function in the CA1 region of the hippocampal slice. Brain Res. 1986;377(2):229-39.

564 42. Baukrowitz T, Yellen G. Modulation of K+ current by frequency and external [K+]: A tale of two
565 inactivation mechanisms. Neuron. 1995;15(4):951-60.

566 43. Nedergaard S. Regulation of Action Potential Size and Excitability in Substantia Nigra Compacta
567 Neurons: Sensitivity to 4-Aminopyridine. Journal of Neurophysiology. 1999;82(6).

568 44. Hoffman AF, Spivak CE, Lupica CR. Enhanced Dopamine Release by Dopamine Transport Inhibitors
569 Described by a Restricted Diffusion Model and Fast-Scan Cyclic Voltammetry. ACS Chem Neurosci.
570 2016;7:700-9.

571 45. Lee TH, Balu R, Davidson C, Ellinwood EH. Differential time-course profiles of dopamine release and
572 uptake changes induced by three dopamine uptake inhibitors. Synapse. 2001;41(4):301-10.

573 46. Stamford JA, Kruk ZL, Millar J. Dissociation of the actions of uptake blockers upon dopamine
574 overflow and uptake in the rat nucleus accumbens: In vivo voltammetric data. Neuropharmacology.
575 1989;28(12):1383-8.

576 47. Sonders MS, Zhu S-J, Zahniser NR, Kavanaugh MP, Amara SG. Multiple Ionic Conductances of the
577 Human Dopamine Transporter: The Actions of Dopamine and Psychostimulants. J Neurosci. 1997;17(3):960-
578 74.

579 48. Acevedo-Rodriguez A, Zhang L, Zhou F, Gong S, Gu H, De Biasi M, et al. Cocaine inhibition of nicotinic
580 acetylcholine receptors influences dopamine release. Front Synaptic Neurosci. 2014;6:19-.

581 49. Zucker RS, Regehr WG. Short-term synaptic plasticity. Ann Review Physiol. 2002;64:355-405.

582 50. Chen C, Regehr WG. Contributions of residual calcium to fast synaptic transmission. J Neurosci.
583 1999;19(15):6257-66.

584 51. Katz B, Miledi R. The role of calcium in neuromuscular facilitation. J Physiol. 1968;195(2):481-92.

585 52. Doussau F, Schmidt H, Dorgans K, Valera AM, Poulain B, Isope P. Frequency-dependent mobilization
586 of heterogeneous pools of synaptic vesicles shapes presynaptic plasticity. Elife. 2017;6.

587 53. Regehr WG. Short-term presynaptic plasticity. Cold Spring Harbor Perspect Biol. 2012;4(7):a005702-
588 a.

589 54. Chung CY, Seo H, Sonntag KC, Brooks A, Lin L, Isacson O. Cell type-specific gene expression of
590 midbrain dopaminergic neurons reveals molecules involved in their vulnerability and protection. Hum Molec
591 Genet. 2005;14(13):1709-25.

592 55. Greene JG, Dingledine R, Greenamyre JT. Gene expression profiling of rat midbrain dopamine
593 neurons: implications for selective vulnerability in parkinsonism. Neurobiol Dis. 2005;18(1):19-31.

594 56. Haber SN, Ryoo H, Cox C, Lu W. Subsets of midbrain dopaminergic neurons in monkeys are
595 distinguished by different levels of mRNA for the dopamine transporter: Comparison with the mRNA for the
596 D2 receptor, tyrosine hydroxylase and calbindin immunoreactivity. J Comp Neurol. 1995;362(3):400-10.

597 57. Blatow M, Caputi A, Burnashev N, Monyer H, Rozov A. Ca2+ Buffer Saturation Underlies Paired Pulse
598 Facilitation in Calbindin-D28k-Containing Terminals. Neuron. 2003;38(1):79-88.

599 58. Felmy F, Neher E, Schneggenburger R. Probing the Intracellular Calcium Sensitivity of Transmitter
600 Release during Synaptic Facilitation. Neuron. 2003;37(5):801-11.

601 59. Stevens CF, Williams JH. Discharge of the Readily Releasable Pool With Action Potentials at
602 Hippocampal Synapses. J Neurophys. 2007;98(6):3221-9.

603 60. Dreyer JK, Herrik KF, Berg RW, Hounsgaard JD. Influence of Phasic and Tonic Dopamine Release on
604 Receptor Activation. J Neurosci. 2010;30(42):14273-83.

605 61. Rooney KE, Wallace LJ. Computational modeling of extracellular dopamine kinetics suggests low
606 probability of neurotransmitter release. Synapse. 2015;69(11):515-25.

607 62. Nanou E, Sullivan JM, Scheuer T, Catterall WA. Calcium sensor regulation of the CaV2.1 Ca2+ channel
608 contributes to short-term synaptic plasticity in hippocampal neurons. Proc Natl Acad Sci USA.
609 2016;113(4):1062-7.

610 63. Sheng J, He L, Zheng H, Xue L, Luo F, Shin W, et al. Calcium-channel number critically influences
611 synaptic strength and plasticity at the active zone. Nat Neurosci. 2012;15(7):998-1006.

612 64. Xu J, Wu L-G. The decrease in the presynaptic calcium current is a major cause of short-term
613 depression at a calyx-type synapse. Neuron. 2005;46(4):633-45.

614 65. He Y, Zorumski CF, Mennerick S. Contribution of Presynaptic Na+ Channel Inactivation to Paired-
615 Pulse Synaptic Depression in Cultured Hippocampal Neurons. J Neurophysiol. 2002;87(2):925-36.

616 66. Geiger JRP, Jonas P. Dynamic Control of Presynaptic Ca2+ Inflow by Fast-Inactivating K+ Channels in
617 Hippocampal Mossy Fiber Boutons. Neuron. 2000;28(3):927-39.

618 67. Ishikawa T, Nakamura Y, Saitoh N, Li W-B, Iwasaki S, Takahashi T. Distinct Roles of Kv1 and Kv3
619 Potassium Channels at the Calyx of Held Presynaptic Terminal. J Neurosci. 2003;23(32):10445-53.

620 68. Kawaguchi S-y, Sakaba T. Control of inhibitory synaptic outputs by low excitability of axon terminals
621 revealed by direct recording. Neuron. 2015;85(6):1273-88.

622 69. Ueda A, Wu C-F. Distinct Frequency-Dependent Regulation of Nerve Terminal Excitability and
623 Synaptic Transmission by IA and IK Potassium Channels Revealed by Drosophila Shaker and Shab Mutations. J
624 Neurosci. 2006;26(23):6238-48.

625 70. Bolam JP, Pissadaki EK. Living on the edge with too many mouths to feed: Why dopamine neurons
626 die. Mov Disord. 2012;27(12):1478-83.

627 71. Ofer N, Shefi O, Yaari G. Branching morphology determines signal propagation dynamics in neurons.
628 Scientific Reports. 2017;7(1):8877-.

629 72. Brody DL, Yue DT. Release-Independent Short-Term Synaptic Depression in Cultured Hippocampal
630 Neurons. J Neurosci. 2000;20(7):2480-94.

631 73. Debanne D, Campanac E, Bialowas A, Carlier E, Alcaraz G. Axon physiology. Physiol Rev.
632 2011;91(2):555-602.

633 74. Pacelli C, Giguère N, Bourque M-J, Lévesque M, Slack Ruth S, Trudeau L-É. Elevated Mitochondrial
634 Bioenergetics and Axonal Arborization Size Are Key Contributors to the Vulnerability of Dopamine Neurons.
635 Current Biology. 2015;25(18):2349-60.

636 75. Jones SR, Gainetdinov RR, Wightman RM, Caron MG. Mechanisms of amphetamine action revealed
637 in mice lacking the dopamine transporter. Journal of Neuroscience. 1998;18(6):1979-86.

638 76. Mateo Y, Budygin EA, John CE, Banks ML, Jones SR. Voltammetric assessment of dopamine clearance
639 in the absence of the dopamine transporter: no contribution of other transporters in core or shell of nucleus
640 accumbens. J Neurosci Meth. 2004;140(1-2):183-7.

641 77. Gu H, Wall SC, Rudnick G. Stable expression of biogenic amine transporters reveals differences in
642 inhibitor sensitivity, kinetics, and ion dependence. J Biol Chem. 1994;269(10):7124-30.

643 78. McElvain JS, Schenk JO. A multisubstrate mechanism of striatal dopamine uptake and its inhibition
644 by cocaine. Biochem Pharmacol. 1992;43(10):2189-99.

645 79. Cameron KN, Solis E, Ruchala I, De Felice LJ, Eltit JM. Amphetamine activates calcium channels
646 through dopamine transporter-mediated depolarization. Cell Calcium. 2015;58(5):457-66.

647 80. Smith DO. Mechanisms of action potential propagation failure at sites of axon branching in the
648 crayfish. J Physiol. 1980;301:243-59.

649 81. Maiya R, Ponomarev I, Linse KD, Harris RA, Mayfield RD. Defining the dopamine transporter
650 proteome by convergent biochemical and in silico analyses. Genes Brain Behav. 2007;6(1):97-106.

651 82. Benoit-Marand M, Ballion B, Borrelli E, Boraud T, Gonon F. Inhibition of dopamine uptake by D2
652 antagonists: an in vivo study. J Neurochem. 2011;116(3):449-58.

653 83. Lee FJS, Pei L, Moszczynska A, Vukusic B, Fletcher PJ, Liu F. Dopamine transporter cell surface
654 localization facilitated by a direct interaction with the dopamine D2 receptor. EMBO J. 2007;26(8):2127-36.

655 84. Martel P, Leo D, Fulton S, Bérard M, Trudeau L-E. Role of Kv1 potassium channels in regulating
656 dopamine release and presynaptic D2 receptor function. PLoS One. 2011;6(5):e20402-e.

657 85. Nirenberg MJ, Vaughan RA, Uhl GR, Kuhar MJ, Pickel VM. The dopamine transporter is localized to
658 dendritic and axonal plasma membranes of nigrostriatal dopaminergic neurons. Journal of Neuroscience.
659 1996;16(2):436-47.

660 86. Suaud-Chagny MF. In vivo monitoring of dopamine overflow in the central nervous system by
661 amperometric techniques combined with carbon fibre electrodes. Methods. 2004;33(4):322-9.

662 87. Marshall JF, O'Dell SJ, Navarrete R, Rosenstein AJ. Dopamine high-affinity transport site topography
663 in rat brain: Major differences between dorsal and ventral striatum. Neuroscience. 1990;37(1):11-21.

664 88. Exley R, McIntosh JM, Marks MJ, Maskos U, Cragg SJ. Striatal alpha5 nicotinic receptor subunit
665 regulates dopamine transmission in dorsal striatum. J Neurosci. 2012;32(7):2352-6.

666 89. Kume-Kick J, Rice ME. Dependence of dopamine calibration factors on media Ca2+ and Mg2+ at
667 carbon-fiber microelectrodes used with fast-scan cyclic voltammetry. J Neurosci Meth. 1998;84(1-2):55-62.

668 90. Agus ZS, Kelepouris E, Dukes I, Morad M. Cytosolic magnesium modulates calcium channel activity in
669 mammalian ventricular cells. Am J Physiol - Cell Physiol. 1989;256(2).

670 91. Lansman JB, Hess P, Tsien RW. Blockade of current through single calcium channels by Cd2+, Mg2+,
671 and Ca2+. Voltage and concentration dependence of calcium entry into the pore. J Gen Physiol.
672 1986;88(3):321-47.

673 92. van der Westhuizen ET, Valant C, Sexton PM, Christopoulos A. Endogenous allosteric modulators of
674 G protein-coupled receptors. J Pharmacol Exp Therapeut. 2015;353(2):246-60.

675 93. Berggård T, Miron S, Onnerfjord P, Thulin E, Åkerfeldt KS, Enghild JJ, et al. Calbindin D28k Exhibits
676 Properties Characteristic of a Ca2+ Sensor. J Biol Chem. 2002;277(19):16662-72.

677 94. Michailova A, McCulloch AD. Model Study of ATP and ADP Buffering, Transport of Ca2+ and Mg2+,
678 and Regulation of Ion Pumps in Ventricular Myocyte. Biophys J. 2001;81:614-29.

679 ## Figure Legends

680 **Figure 1. Short-term plasticity at DA release sites is region-specific and only weakly release-dependent.**
681 **(A, B)** Mean profiles of $[DA]_o$ transients (± SEM) elicited by single or paired electrical pulses at IPI of 10-200 ms
682 in CPu (A, *n* = 4) and NAc (B, *n* = 3). Dotted traces, $[DA]_o$ attributable to the second pulse, P2, in a pair (P1+P2
683 – P1). **(C)** Mean P2/P1 (± SEM) vs. IPIs in CPu (*filled circles*) and NAc (*open circles*). **(D)** P2/P1 vs peak 1p-evoked
684 $[DA]_o$ for IPIs of 10 ms (*left*), 40 ms (*centre*) and 100 ms (*right*). Each data point is 1 site in CPu (*filled circles*, *n*
685 = 35) or NAc (*open circles*, *n* = 19). Linear fits to data show *P*-values (F-test) to indicate whether the slope is
686 significantly > 0. **(E,F)** (*Left)* Mean profiles of $[DA]_o$ transients in CPu (E, *n* = 5) and NAc (F, *n* = 6) in control
687 conditions vs L741,626 (1 µM, *green*). (*Right*) Mean P2/P1 vs IPIs in control conditions and L741,626 in CPu (E)
688 or NAc (F). Two-way ANOVA with Bonferroni's test for *post-hoc* comparisons: **P* < 0.05, ***P* < 0.01.

689 **Figure 2. STP is shaped by release-dependent facilitation and release-independent depression. (A, B)** Mean
690 profiles of $[DA]_o$ transients (± SEM) evoked by single or paired electrical pulses in 1.2 mM (*light grey*), 2.4 mM
691 (*dark grey*) and 3.6 mM (*black*) $[Ca^{2+}]_o$ in CPu (A, *n* = 3) and NAc (B, *n* = 3). **(C)** Mean 1p evoked $[DA]_o$ (± SEM,
692 normalised to 2.4 mM $[Ca^{2+}]_o$) vs $[Ca^{2+}]_o$ in CPu (*filled*) and NAc (*open circles*). **(D, E)** Mean P2/P1 (± SEM) vs. IPI
693 in 1.2 mM (*light grey*), 2.4 mM (*dark grey*) and 3.6 mM (*black*) $[Ca^{2+}]_o$ in CPu (D, *filled*) and NAc (D, *open circles*).
694 **(F)** Mean P2/P1 (± SEM) vs mean peak 1p $[DA]_o$ (± SEM) at 10 ms IPI in 1.2 mM (*light grey*), 2.4 mM (*dark grey*)
695 and 3.6 mM (*black*) $[Ca^{2+}]_o$ in CPu (*filled*) and NAc (*open circles*). **(G)** Mean profiles of $[DA]_o$ transients (± SEM)
696 elicited by single or paired light pulses at 40 ms IPI (473 nm, 2 ms) in 1.0 mM (*light grey*), 2.0 mM (*dark grey*)
697 and 3.0 mM (*black*) $[Ca^{2+}]_o$ in CPu (*left*, *n* = 3) and NAc (*right*, *n* = 3). **(H)** Mean peak 1p $[DA]_o$ (± SEM, normalised
698 to 2.4 mM $[Ca^{2+}]_o$) vs $[Ca^{2+}]_o$ evoked by light stimulation in CPu (*filled*) and NAc (*open circles*). Second-order
699 polynomial curve fit; F-test of relative sum of squares shows curve fits are different. **(I)** Mean P2/P1 (± SEM)
700 at 40 ms IPI vs mean peak 1p $[DA]_o$ (± SEM) evoked by optical stimulation in CPu (*filled*) and NAc (*open circles*).
701 Two-way ANOVA with Bonferroni's test for *post-hoc* comparisons except where stated otherwise: **P* < 0.05,
702 ***P* < 0.01, ****P* < 0.001.

703 **Figure 3. A release-insensitive mechanism of short-term depression is controlled by [K^+]-dependent gating.**
704 **(A, B)** Mean profiles of $[DA]_o$ (± SEM) elicited by single or paired electrical pulses in 1.25 mM (*light grey*), 5 mM
705 (*dark grey*) and 7.5 mM $[K^+]_o$ (*black*) in CPu (A, *n* = 3) and NAc (B, *n* = 3). **(C, D)** Mean P2/P1 (± SEM) vs IPIs in
706 1.25 mM (*light grey*), 5 mM (*dark grey*) and 7.5 mM $[K^+]_o$ (*black*) in CPu (C) and NAc (D). **(E)** Mean P2/P1 (±
707 SEM) vs. mean peak 1p $[DA]_o$ (± SEM) in 1.25 mM (*light grey*), 5 mM (*dark grey*) and 7.5 mM (*black*) $[K^+]_o$ in
708 CPu (*filled*) and NAc (*open circles*) at 10 ms IPI (*left*) and 100 ms IPI (*right*). Two-way ANOVA with Bonferroni's
709 test for *post-hoc* comparisons; *$P < 0.05$, ***$P < 0.001$.

710 **Figure 4. K^+-dependent gating of short-term depression requires axonal Kv channels. (A, E)** Mean profiles of
711 $[DA]_o$ transients (± SEM) in CPu elicited by single or paired electrical pulses in control conditions (*black*) or with
712 100 µM 4-AP (*grey*) in CPu (A, *n* = 4) and NAc (E, *n* = 3). Vertical scale is normalised to peak 1p $[DA]_o$ in control
713 conditions. **(B, F)** Mean 1p $[DA]_o$ (± SEM) in CPu in 1 mM and 5 mM $[K^+]_o$ in control conditions (*black*) or 4-AP
714 (*grey*) in CPu (B) or in NAc (F). **(C, G)** Mean P2/P1 (± SEM) in CPu vs IPI in 5 mM (*black*) and 1 mM (*grey*) $[K^+]_o$
715 in control conditions (*left*) and 4-AP (*right*) in CPu (C) and in NAc (G). **(D, H)** Mean P2/P1 (± SEM) in CPu at 25
716 ms IPI in 1 mM and 5 mM $[K^+]_o$ in control conditions (*black*) or 4-AP (*grey*) in CPu (D) and in NAc (H). (D),
717 asterisks indicate interaction between $[K^+]_o$ and 4-AP. Two-way ANOVA with Bonferroni's test for *post-hoc*
718 comparisons; *$P < 0.05$, **$P < 0.01$.

719 **Figure 5. K^+-dependent gating does not alter release-dependence of STP. (A,B,E,F)** Mean profiles of $[DA]_o$
720 transients (± SEM) elicited by single or paired pulses in 1.2 mM $[Ca^{2+}]$ (*light grey*), 2.4 mM $[Ca^{2+}]_o$ (*dark grey*)
721 and 3.6 mM $[Ca^{2+}]_o$ (*black*) in either 5 mM $[K^+]_o$ (*A,E*) or 1 mM $[K^+]_o$ (*B,F*) in CPu (A,B, *n* = 11) and in NAc (E,F, *n*
722 = 7). **(C, G)** Mean peak 1p $[DA]_o$ (± SEM, normalised to 2.4 mM $[Ca^{2+}]_o$) in 5 mM $[K^+]_o$ (*black*) and 1 mM $[K^+]_o$
723 (*grey*) in CPu (C) and in NAc (G). **(D, H)** Mean P2/P1 (± SEM) at 10 ms IPI (*left*) and 100 ms IPI (*right*) in 5 mM
724 $[K^+]_o$ (*black*) and 1 mM $[K^+]_o$ (*grey*) in CPu (D) and in NAc (H). Two-way ANOVA with Bonferroni's test for *post-*
725 *hoc* comparisons.

726 **Figure 6. The dopamine transporter regulates STP of dopamine release. (A, G)** Mean profiles of $[DA]_o$
727 transients (± SEM) elicited by single or paired electrical pulses in control conditions (*black*) or with 5 µM
728 cocaine (*blue*) in CPu (A, *n* = 4) or NAc (G, *n* = 4). **(B, H)** Mean P2/P1 (± SEM) against IPI in control conditions
729 (*black*) and with cocaine (*blue*) in CPu (B) or NAc (H). **(C, I)** Mean profiles of $[DA]_o$ transients (± SEM) elicited by
730 single or paired electrical pulses in control conditions (*black*) or with 5 µM methylphenidate (*MPH*, *grey*) in
731 CPu (C, *n* = 5) or NAc (G, *n* = 3). **(D, J)** Mean P2/P1 (± SEM) vs IPI in control conditions (*black*) and with MPH
732 (*green*) in CPu (D) or NAc (J). **(E)** Mean profiles of $[DA]_o$ transients (± SEM) elicited by single or paired electrical
733 pulses in control conditions (*black*) or with 10 µM nomifensine (*red*) in CPu (*n* = 3). **(F)** Mean P2/P1 (± SEM) vs
734 IPI in control conditions (*black*) and with nomifensine (*red*) in CPu. Two-way ANOVA with Bonferroni's test for
735 *post-hoc* comparisons; **P* < 0.05, ***P* < 0.01, ****P* < 0.001.

736 **Figure 7. The DAT limits release-dependence of STP in CPu. (A)** Mean profiles of $[DA]_o$ transients (± SEM,
737 vertical scale normalised to 1p in 2.4 mM $[Ca^{2+}]_o$) (*n* = 4) elicited by single or paired electrical pulses in 2.4 mM
738 (*upper*) and 1.2 mM $[Ca^{2+}]_o$ (*lower*) in control conditions (*black*) or 5 µM cocaine (*blue*). **(B, C)** Mean P2/P1 (±
739 SEM) vs. IPI in 1.2 mM (*light*) and 2.4 mM $[Ca^{2+}]_o$ (*dark*) in control conditions (B) or cocaine (C). **(D)** Mean P2/P1
740 (± SEM) in 1.2 mM and 2.4 mM $[Ca^{2+}]_o$ in control conditions (*black-grey*) or cocaine (*blue*) at 25 ms IPI (*left*) or
741 40 ms IPI (*right*). Two-way ANOVA with Bonferroni's test for *post-hoc* comparisons; **P* < 0.05, ***P* < 0.01, ****P*
742 < 0.001.

743 **Figure 8. The DAT and $[K^+]_o$ gate STP through overlapping mechanisms. (A, E)** Mean profiles of $[DA]_o$
744 transients (± SEM) elicited by single or paired electrical pulses in control conditions or cocaine in 5 mM $[K^+]_o$
745 (*upper*) and 1 mM $[K^+]_o$ (*lower*) in CPu (A, *n* = 4) and in NAc (E, *n* = 3). **(B, F)** Mean P2/P1 (± SEM) vs. IPI in 5 mM
746 $[K^+]_o$ (*black*) and 1 mM $[K^+]_o$ (*grey*) in control conditions (*left*) or cocaine (*right*) in CPu (B) and in NAc (F). **(C, G)**
747 Mean 1p $[DA]_o$ (± SEM) in control conditions (*black-grey*) or cocaine (*blue*) in CPu (C) and in NAc (G). **(D, H)**
748 Mean P2/P1 (± SEM) in CPu at 25 ms IPI in 1 mM and 5 mM $[K^+]_o$ in control conditions or with cocaine in CPu
749 (D) and in NAc (H). Two-way ANOVA with Bonferroni's test for *post-hoc* comparisons; **P* < 0.05, ***P* < 0.01.

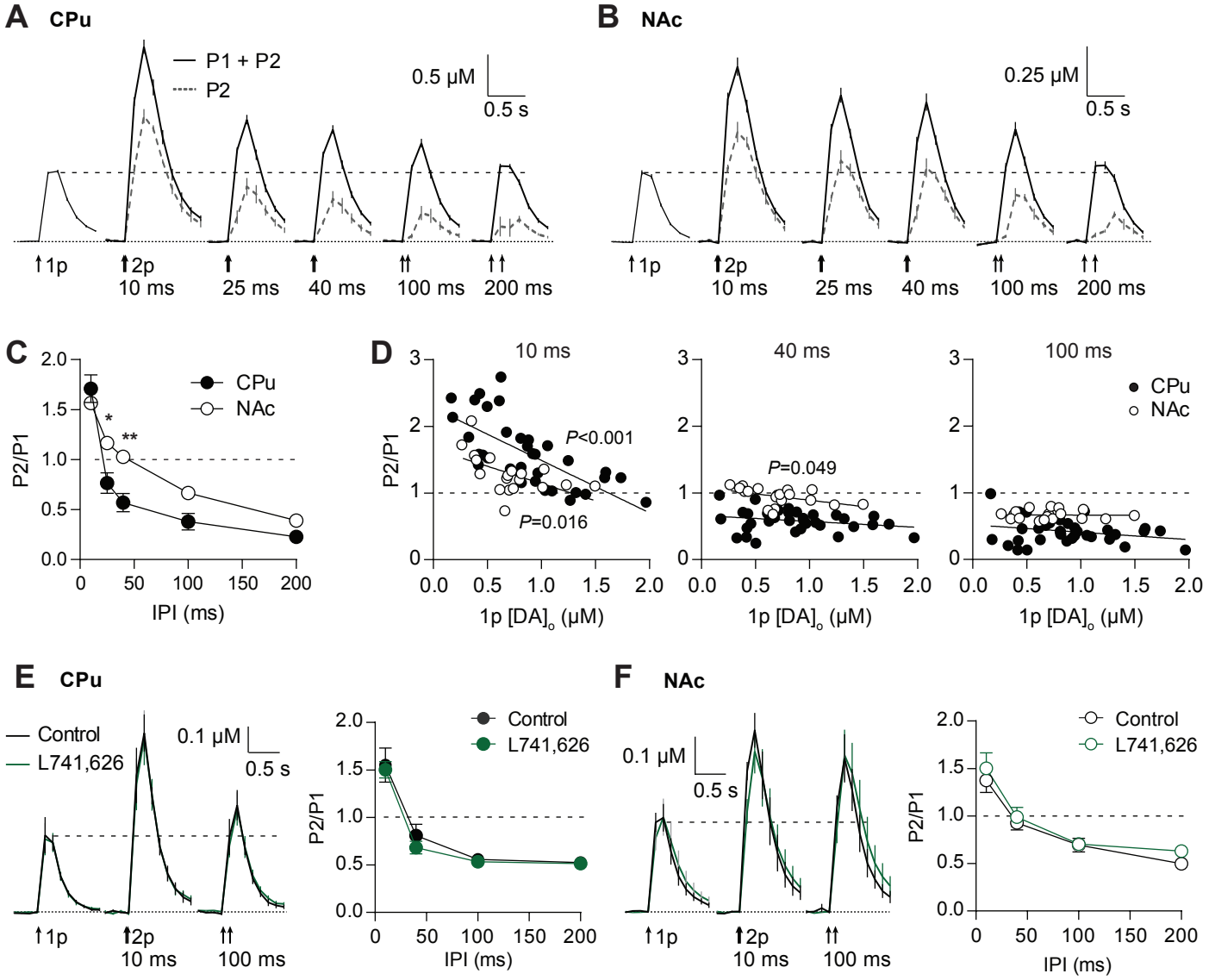

Figure 1
Condon et al

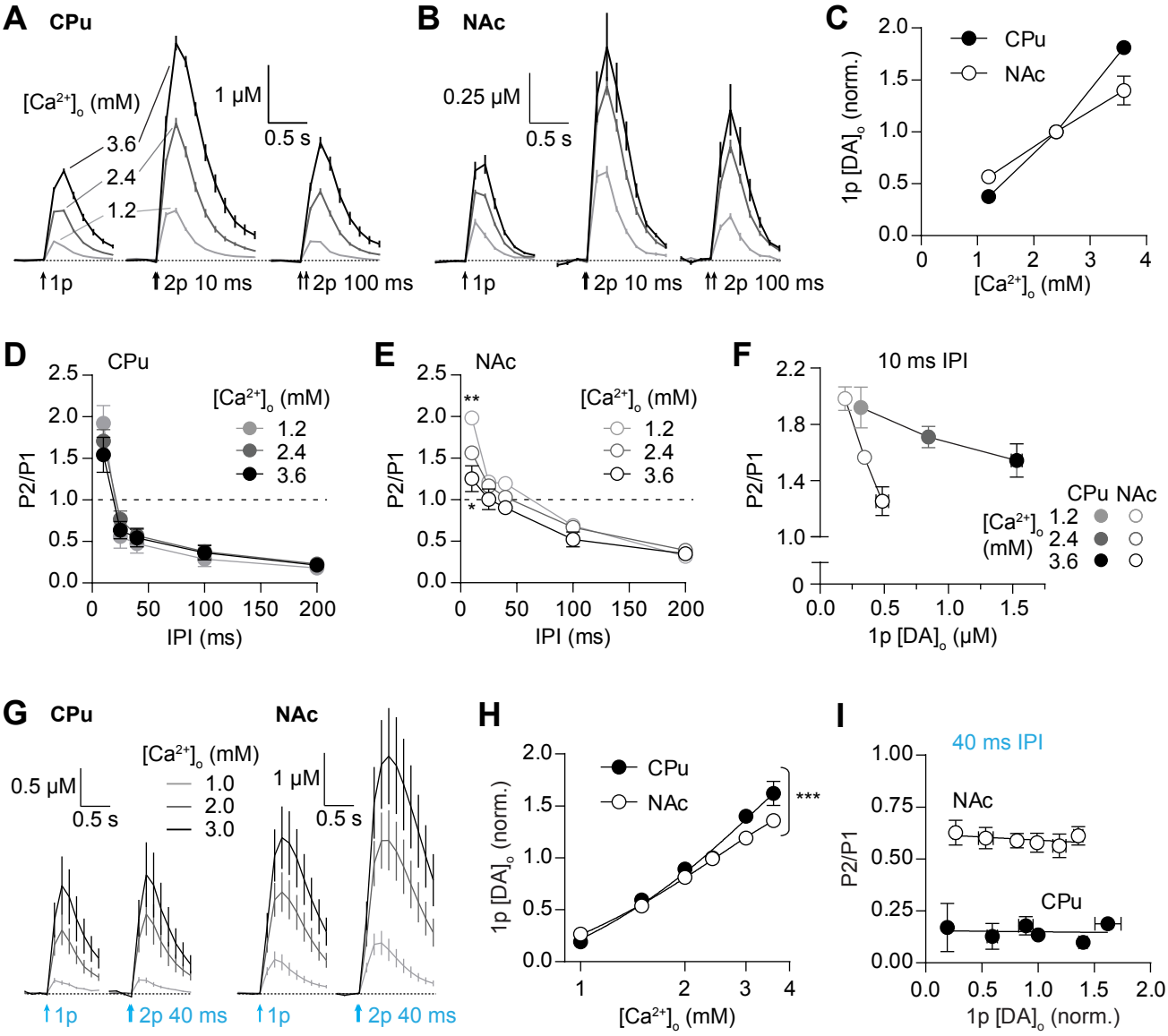

Figure 2
Condon et al

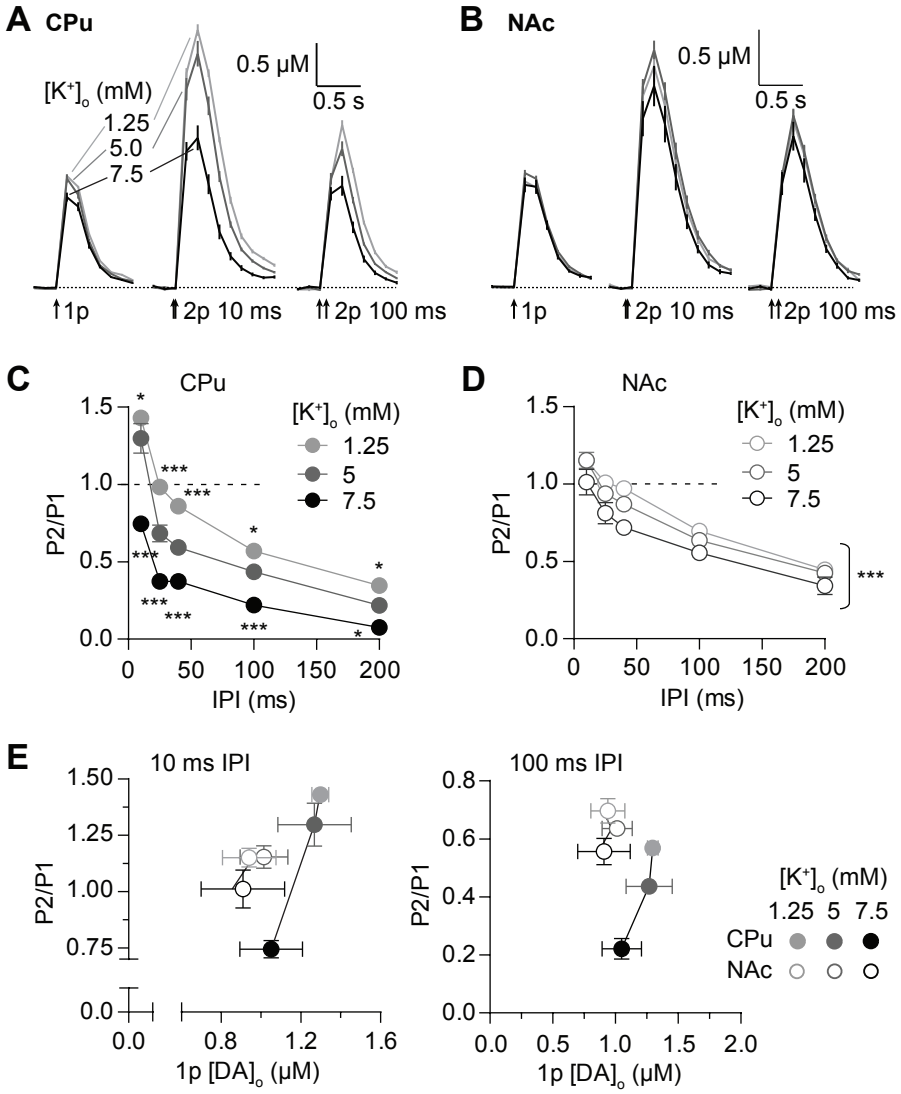

Figure 3
Condon et al

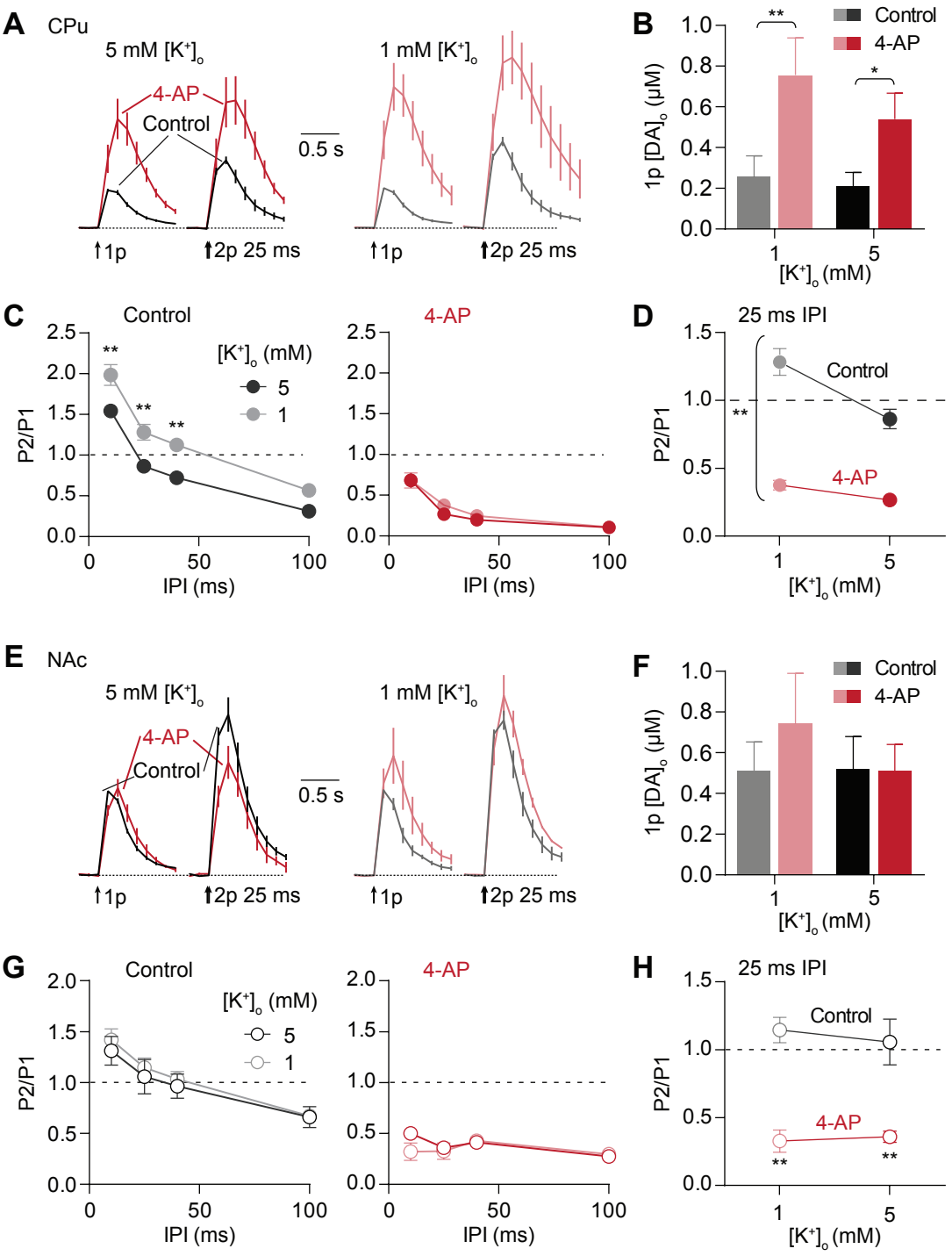

Figure 4
Condon et al

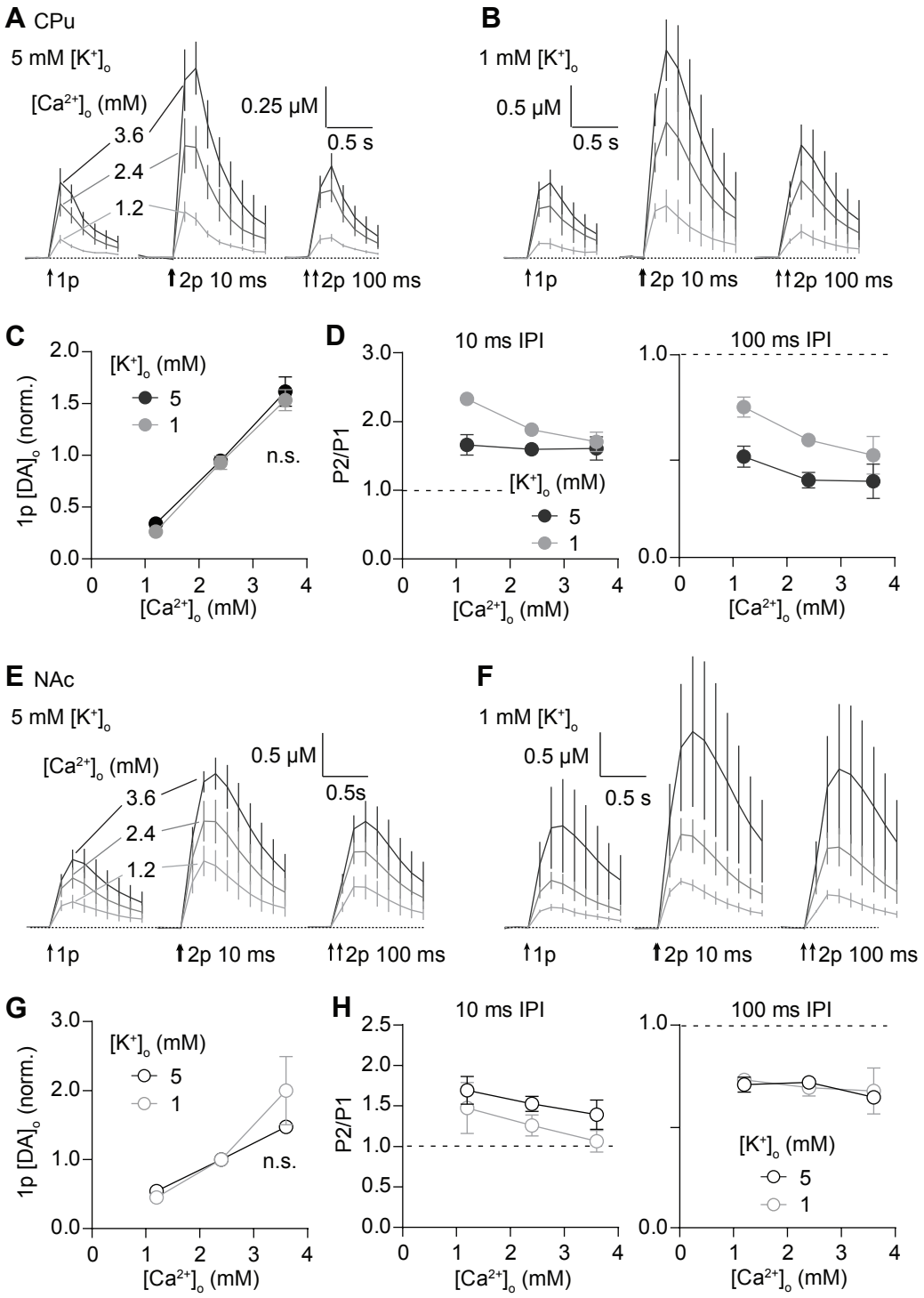

Figure 5
Condon et al

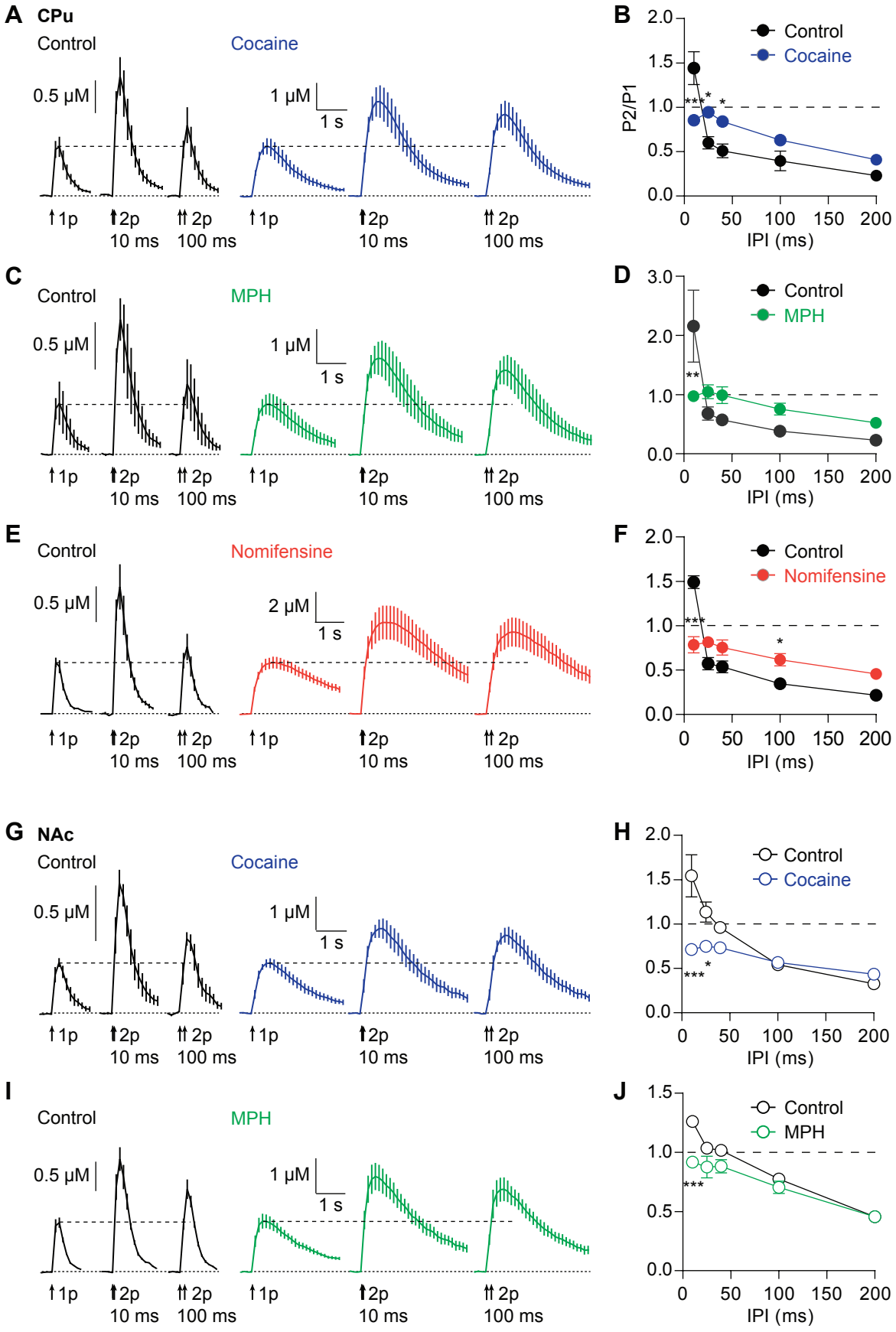

Figure 6
Condon et al

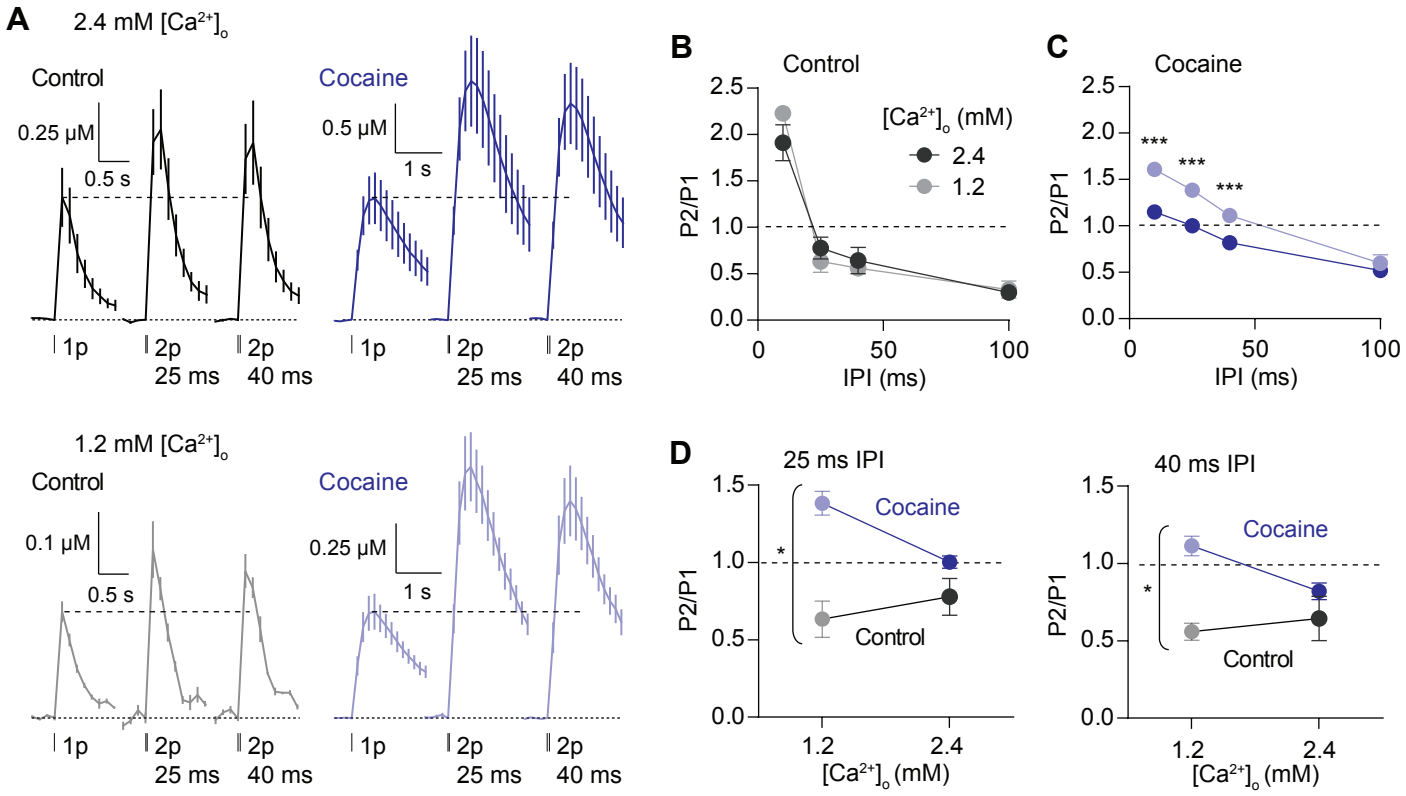

Figure 7
Condon et al

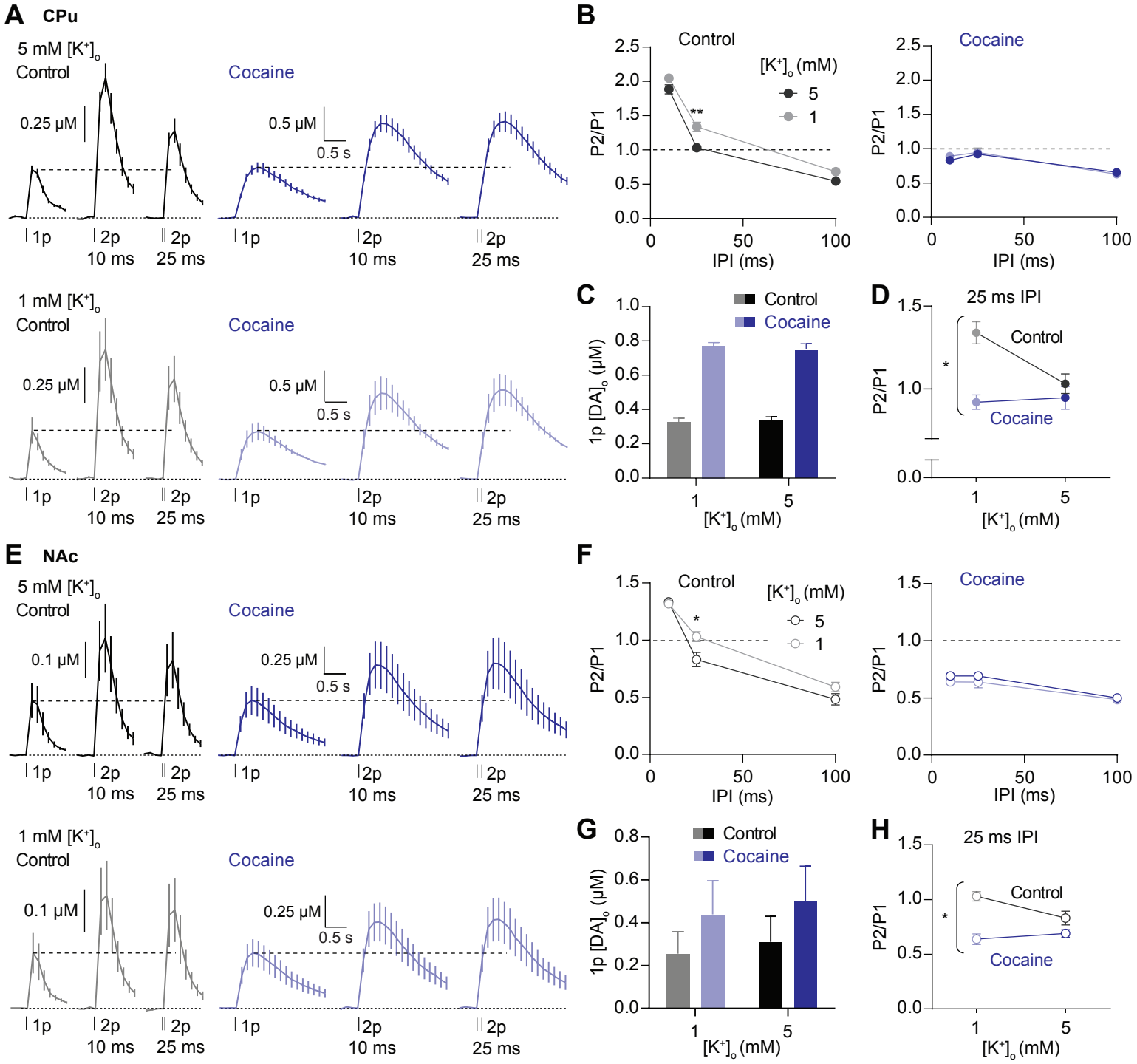

Figure 8
Condon et al

Supporting Data

Figures S1-S4 and Legends

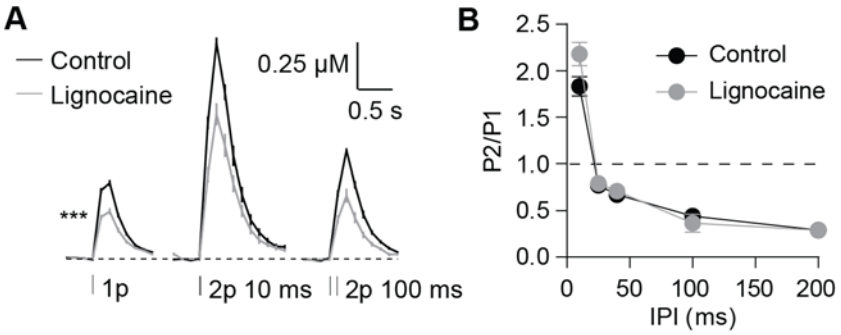

Figure S1. Voltage-gated Na^+ channel inhibitor lignocaine does not replicate the effects of cocaine on STP in CPu

(A) Mean profiles of $[DA]_o$ transients (± SEM) evoked by electrical stimulation in control conditions (*black*) or in the presence of 5 µM lignocaine (*grey*) in CPu (n = 3). Lignocaine significantly decreased 1p $[DA]_o$ (p < 0.001, n = 3). **(B)** Mean P2/P1 ±SEM vs. IPI in control conditions (*black*) or in the presence of lignocaine (*grey*).

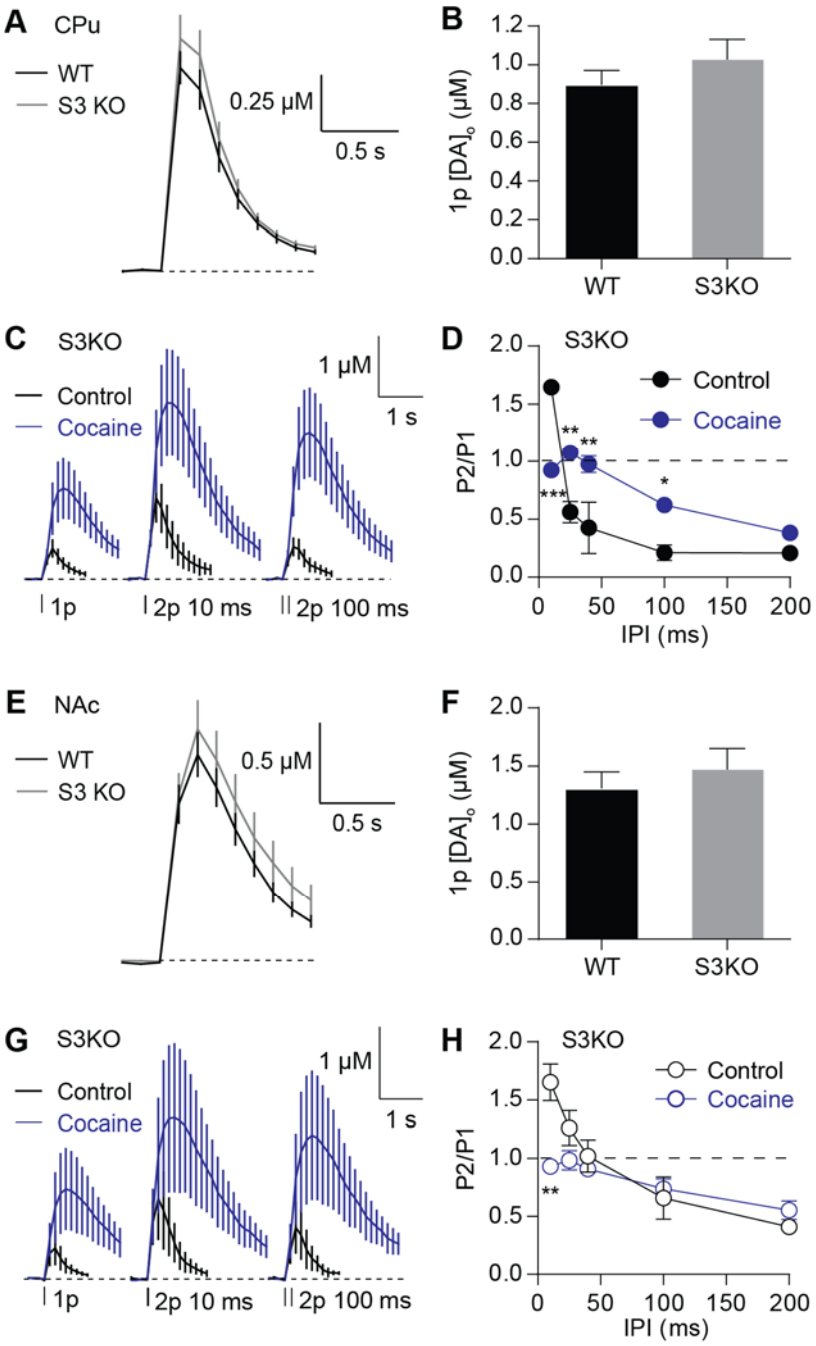

Figure S2. The effects of cocaine on STP are not dependent on synapsin III

(A, E) Mean profiles of $[DA]_o$ transients (± SEM) evoked by single pulses in slices from wild-type (*black*) and S3KO (*grey*) animals in CPu (A, n = 6) and in NAc (E, n = 6). **(B, F)** Mean peak $[DA]_o$ (± SEM) following single pulses in wild-type (*black*) or S3KO (*grey*) animals in CPu (B) and in NAc (F). **(C, G)** Mean profiles of $[DA]_o$ transients (± SEM) evoked by single or paired pulses in control conditions (*black*) or cocaine (*blue*) in S3KO animals in CPu (C) or in NAc (G). **(D, H)** Mean P2/P1 (± SEM) vs. IPIs in control conditions (*black*) or in cocaine (*blue*) in CPu (D) and in NAc (H). Two-way ANOVA with Bonferroni's test for *post-hoc* comparisons; *$P < 0.05$, ** $P < 0.01$, *** $P < 0.001$.

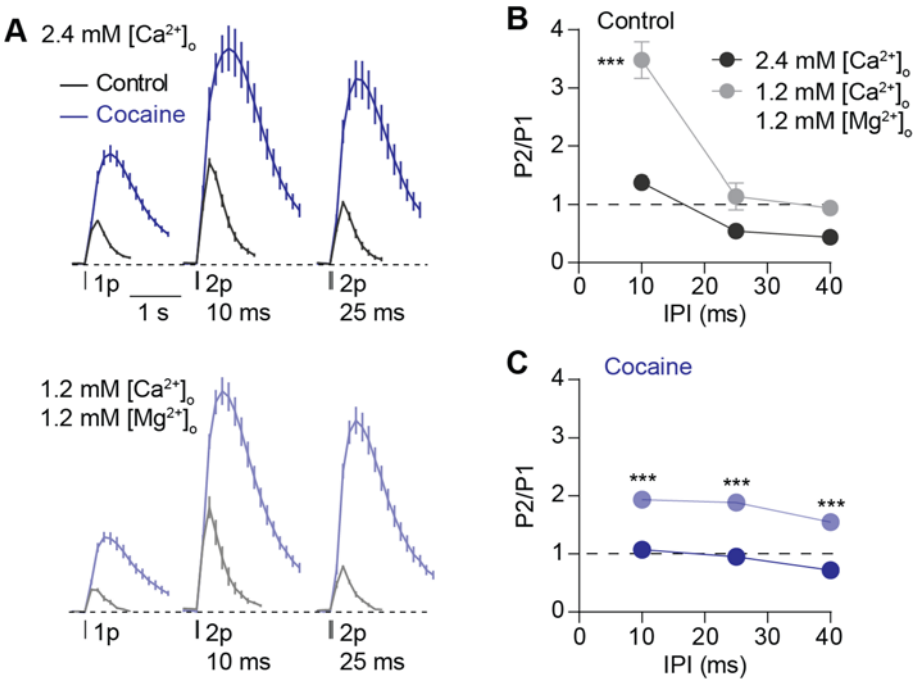

Figure S3. The response to $[Ca^{2+}]_o$ revealed after DAT inhibition (see Fig. 7) is not caused by a change in the extracellular concentration of divalent cations

(A) Mean profiles of $[DA]_o$ transients (± SEM, vertical scale normalised to 1p in 2.4 mM $[Ca^{2+}]_o$) (n = 4) elicited by single or paired electrical pulses in 2.4 mM $[Ca^{2+}]_o$ (*upper*) and 1.2 mM $[Ca^{2+}]_o$ with 1.2 mM $[Mg^{2+}]_o$ (*lower*) in control conditions (*black*) or 5 µM cocaine (*blue*). **(B, C)** Mean P2/P1 (± SEM) vs. IPI in 1.2 mM (*light*) and 2.4 mM $[Ca^{2+}]_o$ (*dark*) in control conditions (B) or cocaine (C). *** P<0.001.

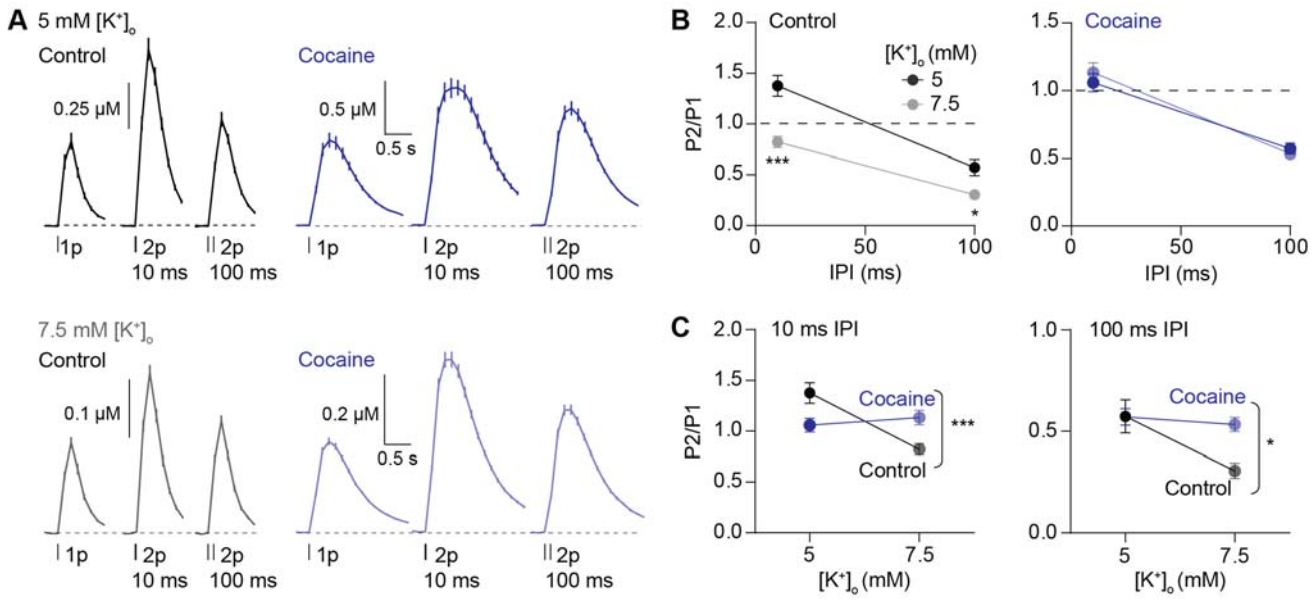

Figure S4. Cocaine prevents enhancement of STD by increased $[K^+]_o$

(A) Mean profiles (± SEM) of $[DA]_o$ transients in 5 mM (*upper*) and 7.5 mM $[K^+]_o$ (*lower*) in control conditions (*black-grey*) and in cocaine (*blue*). **(B)** Mean P2/P1 (± SEM) at IPIs of 10 ms and 100 ms in control conditions (*left*) and in cocaine (*right*) in 5 mM (*dark*) and 7.5 mM (*light*) $[K^+]_o$. **(C)** Mean P2/P1 (± SEM) in CPu at 10 ms IPI (*left*) and 100 ms IPI (*right*) in 5 mM and 7.5 mM $[K^+]_o$ in control conditions (*black-grey*) or with cocaine (*blue*). Two-way ANOVA with Bonferroni's test for *post-hoc* comparisons; * $P < 0.05$, *** $P < 0.001$.